National University of Singapore
PC4199 Honours Project in Physics

Bell Inequalities and Entanglement Witnesses Using Two-Body Correlations

By:
Tan Ying Zhe Ernest (A0003918J)

Supervisors:
Kwek Leong Chuan
Dagomir Kaszlikowski

Abstract

It has been shown that there exist Bell inequalities constructed from symmetric one- and two-body correlations that are violated by certain quantum states involving any number of particles. However, the properties of such Bell inequalities have not been completely characterised. In this study, we determine the behaviour of various classes of entangled states with respect to these inequalities. It is shown that some Dicke states are able to violate such inequalities, and the robustness of the quantum violations against white noise and thermal noise are investigated. Conversely, we show that GHZ states and Smolin states cannot violate such Bell inequalities. We also proceed to develop an entanglement witness based on symmetric two-body correlations, and describe some properties of this entanglement witness. In particular, this entanglement witness is optimal for even numbers of particles. The possibility of relating violation of such inequalities to properties such as entanglement distillation and the Peres-Horodecki criterion is considered.

Acknowledgements

I would like to express my sincere gratitude to my supervisors Prof. Kwek Leong Chuan and Prof. Dagomir Kaszlikowski for their support and guidance over the course of my project. I would also like to thank Prof. Antonio Acín for helpful correspondence regarding entanglement detection for GHZ states, as well as Prof. Valerio Scarani for our fruitful discussions regarding the relations between different entanglement-related properties as well as the possibility of measuring symmetric two-body correlations experimentally.

In addition, thank you to all my friends and family members for the unceasing support you have provided, both over the course of the past year as well as all the rest of the time I have spent in NUS. This would not have been possible without your help.

Contents

List of Figures

List of Tables

Chapter 1

Introduction

In 1964, John Bell developed a theorem that revealed some critical properties of the theory of quantum mechanics [1]. Bell showed that certain results from quantum theory would be incompatible with any physical theory that satisfied several seemingly-intuitive assumptions, most notably those of locality and realism. His theorem took the form of an inequality that had to be satisfied by all local realistic theories, but which would be violated according to quantum mechanics. The finding was particularly significant because many physicists at the time were uncomfortable with the existing interpretations of quantum theory, and sought to disprove it or account for its results in terms of more intuitive physical theories instead. Bell's result showed that any attempt to do so via a local realistic model would be unsuccessful, and also provided in principle an experimental test to verify whether the predictions of quantum mechanics would be borne out.

Since the development of Bell's theorem, a wide range of experiments have been conducted to determine whether nature followed quantum-mechanical predictions or stayed within the constraints of local realistic models [2–5]. Thus far, the results have proven to be in favour of the former. There remains an issue of the fact that there exist several loopholes which prevent one from conclusively ruling out all local realistic models, with no experiment to date having simultaneously addressed all such loopholes. However, these loopholes have been individually addressed in various experiments [3,4], and various approaches have been suggested to achieve progress towards a loophole-free Bell experiment [5]. Realisation of such an experiment would also help to pave the way towards further development of some proposed applications of Bell inequality violation, such as device-independent cryptography.

Depending on the system in consideration, a wide variety of Bell inequalities can be developed [6–11]. While Bell's original inequality considered a system of two qubits with two possible measurement settings, these subsequent works have generalised the concept to N-particle systems, qudits of dimension $d > 2$, and different types of measurement settings. In a recent work, Tura et al. [12] derived a class of Bell inequalities based on symmetric one- and two-body correlations. Our study aims to characterise some

properties of such Bell inequalities, by determining which states are able to violate these inequalities as well as the robustness of the violation against various forms of noise. We also describe how it can be modified to form an operator able to detect entanglement, known as an entanglement witness. Finally, we consider how violation of this class of Bell inequalities is related to a number of other properties such as entanglement distillation.

1.1 Bell inequalities

Bell inequalities are constraints that must be satisfied by any physical model obeying the assumptions of locality and realism, sometimes also referred to as a "classical" model or local hidden variable model [1, 5]. The locality assumption means that if a pair of parties carry out measurements separated by a spacelike interval, the outcome of one party's measurement cannot be influenced by the other party's choice of measurement or measurement outcome. As for the assumption of realism, this refers to the idea that any observable quantity should have a pre-existing value or probability distribution of values for any possible measurement before the choice of measurement is made. While these might appear to be intuitive properties for a physical theory to possess, Bell's theorem showed that if quantum mechanics were correct, then at least one of these assumptions would have to be abandoned.

Out of the various interpretations of quantum mechanics that have arisen, ranging from the Copenhagen interpretation to the many-worlds hypothesis, some have allowed non-locality while others discard the realism assumption. Another proposal referred to as superdeterminism tackles a third assumption in the model, namely the assumption that the parties are able to choose their measurement settings "freely" [13]. However, superdeterminism is a less commonly accepted interpretation as compared to the others.

It is important to note that despite the locality assumption being forfeited in some interpretations, quantum mechanics still does not allow for superluminal communication [14]. This is because the measurements made by one party are unable to affect the conditional probabilities of the measurements made by a spacelike-separated party in a manner that allows for communication of information, a condition more generally referred to as no-signalling. It is only when the parties come together or otherwise communicate classically that they are able to obtain the data required to show a violation of a Bell inequality.

Bell's inequality, as derived in his 1964 paper [1], considered a singlet state distributed to pair of observers, each of whom performs a spin measurement along some axis. Only three possible measurement axes need to be considered, which we can denote as $\left\{\vec{a}, \vec{b}, \vec{c}\right\}$, with corresponding measurements $\{M_a, M_b, M_c\}$. The measurements are all taken to have dichotomous outcomes, with values ± 1. It is important to note that while these properties are characteristic of qubit measurements in the framework of quantum mechanics,

the derivation of the Bell inequality itself does not make use of results from quantum mechanics, merely requiring that the measurement choices and outcomes satisfy these specific properties along with the assumptions of locality and realism. This therefore allowed Bell to derive a constraint which had to hold for any local realistic physical theory, completely independent of predictions from quantum mechanics.

Bell showed that if the outcomes of the observers' measurements could be accounted for by some local realistic model, their results would have to obey the inequality

$$1 + \left\langle M_b^{(1)} M_c^{(2)} \right\rangle \geq \left| \left\langle M_a^{(1)} M_b^{(2)} \right\rangle - \left\langle M_a^{(1)} M_c^{(2)} \right\rangle \right|, \tag{1.1}$$

where $\left\langle M_\alpha^{(1)} M_\beta^{(2)} \right\rangle$ denotes the mean value of the product of the observers' measurement outcomes obtained when the first observer made a measurement along the $\vec{\alpha}$-axis and the second observer made a measurement along the $\vec{\beta}$-axis. In deriving Eq. (1.1), Bell in fact made use of an additional assumption that the observers' measurement outcomes would be perfectly anticorrelated if both chose the same measurement axis. However, this assumption is not required in general to obtain other bounds on local realistic models, and subsequent works have derived inequalities not requiring this assumption [6]. Bell then noted that for some choices of the directions $\left\{\vec{a}, \vec{b}, \vec{c}\right\}$, for instance such that $\vec{a}.\vec{c} = 0$ and $\vec{a}.\vec{b} = \vec{b}.\vec{c} = 1/\sqrt{2}$, quantum mechanics predicted values that violated the inequality. He hence concluded that quantum mechanics could not be compatible with local realistic models.

Another important Bell inequality was derived by Clauser et al. in 1969, and is now referred to as the Clauser-Horne-Shimony-Holt (CHSH) inequality [6]. It again concerns a pair of observers, with dichotomous measurements having outcomes ± 1. Unlike Eq. (1.1) however, the CHSH inequality can be derived without assuming perfect anticorrelation. The first observer is assumed to have a choice between two measurements $M_0^{(1)}$ and $M_1^{(1)}$, and the second observer's measurement choices are $M_0^{(2)}$ and $M_1^{(2)}$. The CHSH inequality then states

$$\left| \left\langle M_0^{(1)} M_0^{(2)} \right\rangle + \left\langle M_0^{(1)} M_1^{(2)} \right\rangle + \left\langle M_1^{(1)} M_0^{(2)} \right\rangle - \left\langle M_1^{(1)} M_1^{(2)} \right\rangle \right| \leq 2. \tag{1.2}$$

Again, for particular choices of measurement settings and quantum states, this inequality is violated by the predictions of quantum mechanics, with a maximum value of $2\sqrt{2}$ on the left-hand side.

As shown in Eqs. (1.3) and (1.2), Bell inequalities are statements about expectation values, or in some cases probabilities. This therefore means that any experimental attempt to detect violation of Bell inequalities is necessarily of a statistical nature. By conducting multiple trials, these expectation values or probabilities can be estimated from the results. However, for any finite number of trials, it is in principle possible that a local

realistic model could produce results violating a Bell inequality, simply by chance [15]. Experiments investigating Bell inequality violations need to gather enough data to reduce the probability of this chance outcome to some acceptable threshold. The amount of data required to achieve this is a question of finite statistics, which needs to be considered in terms of the assumptions underlying the setup and the goal of the experiment.

We now consider more general Bell inequalities. In general, Bell inequalities may be constructed based on the probabilities or correlations of various measurements and their outcomes. However, in this study we focus only on correlation-based Bell inequalities. Given an N-particle state and a choice of some measurement settings $\left\{M_0^{(i)}, M_1^{(i)}, ...\right\}$ on each particle i, the one- to N-body correlations $\left\{\left\langle M_0^{(i)}\right\rangle, \left\langle M_1^{(i)}\right\rangle, ..., \left\langle M_0^{(i)} M_0^{(j)}\right\rangle, ...\right\}$ can be computed. The one-body terms are not in fact "correlations" in the original sense of the word, but it is expedient to refer to them as such and there is little danger of confusion in doing so. The correlations can then be used to construct Bell inequalities, with a general correlation-based Bell inequality taking the form

$$\sum_{i=1}^{N} \sum_{a \in \mathcal{M}} \alpha_{ai} \left\langle M_a^{(i)} \right\rangle + \sum_{\substack{i,j=1 \\ i \neq j}}^{N} \sum_{\substack{a,b \in \mathcal{M} \\ a \leq b}} \beta_{ai,bj} \left\langle M_a^{(i)} M_b^{(j)} \right\rangle + ... + \sum_{a,b,... \in \mathcal{M}} \omega_{a,b,...} \left\langle M_a^{(1)} M_b^{(2)} ... M_n^{(N)} \right\rangle \leq B_C, \tag{1.3}$$

where $\mathcal{M}$ is the set of labels for the measurement settings, $\alpha_{ai}, \beta_{ai,bj}, ..., \omega_{a,b,...}$ are coefficients for the correlations and B_C is a bound referred to as the classical bound. This bound represents the maximum value that can be obtained in a local realistic model.

The ordered set of one- to N-body correlations $\left(\left\langle M_0^{(1)}\right\rangle, ..., \left\langle M_a^{(1)} M_b^{(2)} ... M_n^{(N)}\right\rangle\right)$ can be viewed as coordinates in a vector space. Eq. (1.3) then defines a region to one side of a hyperplane in this correlation vector space, with the normal to the hyperplane being specified by the coefficients $\alpha_{ai}, \beta_{ai,bj}, ..., \omega_{a,b,...}$. It has been shown that the region defined by all the Bell inequalities for a given system is a polytope in this space [5]; in other words, it is a convex set with only a finite number of extremal points. A finite number of Bell inequalities hence suffices to specify all facets of this polytope, which may be referred to as the classical polytope or local polytope. A number of the facets may be trivial in the sense that they arise merely due to the requirement that all probabilities must be non-negative and sum to 1. For the two-qubit case with two measurement settings per observer, the CHSH inequality is the only non-trivial correlation-based Bell inequality [5].

The vertices of the classical polytope correspond to deterministic local realistic models, in which all correlations factorise and all expectation values $\left\langle M_a^{(i)}\right\rangle$ are equal to one of the possible measurement outcomes [5]. For instance, in the case where all measurements are dichotomous measurements with possible outcomes ± 1, the vertices are given by listing the possible combinations of expectation values such that $\left\langle M_a^{(i)}\right\rangle = \pm 1$, with all

higher-order correlations being specified by $\left\langle M_a^{(i)} M_b^{(j)} ... \right\rangle = \left\langle M_a^{(i)} \right\rangle \left\langle M_b^{(j)} \right\rangle ...$ and so on.

For any given set of coefficients in Eq. (1.3), it is possible in principle to obtain the classical bound B_C by enumerating all the vertices and taking the maximum over the vertices. However, this method is computationally inefficient since the number of vertices increases rapidly with N. For instance, for an N-particle system with m choices of measurement settings each with d possible outcomes, a direct enumeration of all the deterministic local realistic models yields d^{mN} combinations. Therefore, the wide variety of Bell inequalities that have been studied [6–11] typically focus on cases where a simple expression or value can be found for the bound, usually with the coefficients and bound defining some facet of the classical polytope.

If a Bell inequality is violated by a quantum state that gives some value Q on the left-hand side of Eq. (1.3), the quantity $(Q - B_C)/B_C = Q/B_C - 1$ expresses how much the quantum value exceeds the classical bound, relative to the classical bound. This shall be referred to as the relative quantum violation. If the measurement settings are chosen such that the expectation values of all correlations for the maximally mixed state $\mathbb{I}/2^N$ are zero, the relative quantum violation provides a measure of the robustness of the Bell inequality violation against white noise, in that if some state ρ has a relative quantum violation of q, then adding white noise to the state ρ in the form

$$\rho_{\text{whitenoise}} = P\rho + (1 - P)\,\frac{\mathbb{I}}{2^N} \tag{1.4}$$

causes it to no longer violate the Bell inequality when $(1-P) > \frac{q}{q+1}$. Therefore, the larger the relative quantum violation q, the greater the fraction $(1 - P)$ of white noise that can be added before the state no longer violates the Bell inequality. In terms of the correlation space, the quantum violation $(Q - B_C)$ for some state violating a Bell inequality gives the distance between the state's position in correlation space and the facet of the classical polytope corresponding to that Bell inequality. Adding white noise causes the state's position to move linearly towards the origin, with the point where it enters the classical polytope being the point where it ceases to violate that Bell inequality.

The set of points in correlation space that can be achieved by quantum states is also demarcated by some bounds of its own, known as Cirel'son inequalities [16]. As previously mentioned, although this set can violate the Bell inequalities constraining local realistic models, it stays within bounds imposed by a requirement of no-signalling. It is interesting to note, however, that it is strictly smaller than the set of points that can be attained by no-signalling models. In some sense, quantum correlations do not explore the full extent of correlations that would be accessible if one only requires that a physical theory be non-signalling [14].

The fact that violation of a Bell inequality implies incompatibility with local realism also has consequences that are not necessarily related to quantum mechanics. Apart from

the fact that loophole-free experimental realisations of such violations would demonstrate that nature cannot be described by any local realistic theory, Bell inequality violations have also been considered in attempts to design device-independent protocols [17–19]. This refers to protocols for procedures such as key distribution or randomness generation that can be proven to be secure or otherwise reliable, with only minimal assumptions about the nature of the devices used to implement the protocol. The idea of such proofs broadly relies on the concept that any deterministic non-local model necessarily violates the no-signalling constraint. Therefore, any model that produces correlations incompatible with local realism, but still obeys the no-signalling constraint, should possess some form of intrinsic indeterminism regardless of the exact details of the devices used to implement the protocol. In particular, quantum mechanics is just such a model.

Device-independent protocols hence attempt to use violation of Bell inequalities in order to certify randomness or security, with quantum mechanics allowing such violation to be achieved. A wide variety of such protocols have been developed, using different assumptions for their purposes. An adversary attempting to obtain information from the protocol may be assumed to be constrained either by quantum mechanics or merely by the no-signalling requirement, depending on the procedure in question [17, 19]. Some of the protocols are designed to be secure even if the devices were constructed by the adversary, as long as the devices satisfy some constraints such as not being able to simply broadcast the measurement outcomes to the attacker. The initial results along these lines required some practically infeasible assumptions such as unrealistically low noise levels [17,18], but subsequent works have generalised these procedures to more realistic assumptions such as only restricting the adversary to have limited quantum memory [19].

1.2 Entanglement

Not all quantum states are able to violate Bell inequalities. A necessary but not sufficient condition for a state to violate a Bell inequality is for it to be an entangled state, meaning a state that is not separable. For pure states, a separable state is defined as one that can be expressed as a product of subsystem states,

$$|\psi_{\text{sep}}\rangle = \left|\psi^{(1)}\right\rangle \otimes \left|\psi^{(2)}\right\rangle \otimes ... \otimes \left|\psi^{(N)}\right\rangle . \tag{1.5}$$

For mixed states, a separable state is one that can be expressed as a convex combination of product states,

$$\rho_{\text{sep}} = \sum_{i=1}^{k} p_i \, \rho_i^{(1)} \otimes \rho_i^{(2)} \otimes ... \otimes \rho_i^{(N)}, \quad \text{where } \sum_{i=1}^{M} p_i = 1. \tag{1.6}$$

Without loss of generality, all the $\rho_i^{(j)}$ subsystem states can be taken to be pure. This mixed-state definition encompasses the pure-state definition under the case where $M = 1$ and all the $\rho_i^{(j)}$ subsystem states are pure.

In the case of pure states, it has been shown that a state is entangled if and only if it violates a Bell inequality [20, 21]. On the other hand, there exist entangled mixed states which do not violate any Bell inequalities of the form in Eq. (1.3) by themselves. Techniques such as joint measurements [22] or using a sequence of measurements [23] can sometimes be used to cause such entangled states to violate Bell inequalities, but the exact nature of the relation between entanglement and Bell violations remains elusive. A result by Liang et al. also shows that any entangled state that does not violate a given Bell inequality can be made to violate that inequality by appending an auxiliary state which does not violate that inequality by itself [24].

Apart from Bell inequality violation, entangled states may be useful in a variety of protocols that have been proposed based on quantum theory. For instance, some entangled states can be used for quantum cryptography [25], teleportation [26], or error correction [27]. However, determining whether an arbitrary state is entangled or separable may not be an easy task, as it is not always obvious whether a given state expressed with respect to some basis can be rewritten as a convex combination of product states. Two methods which shall now be described are the use of entanglement witnesses and the Peres-Horodecki criterion. Attempting to find some way to quantify the extent to which a state is entangled has also proven to be a difficult problem, giving rise to a number of entanglement measures which are often related but not equivalent to each other. Some such measures include distillable entanglement and the entanglement of formation, which shall be briefly discussed.

1.2.1 Entanglement witnesses

One method which may be useful in detecting entanglement is the concept of an entanglement witness. An entanglement witness refers to an operator W that has non-negative expectation value $\mathrm{Tr}(W\rho_{\mathrm{sep}}) \geq 0$ for all separable states ρ_{sep}, and negative expectation value $\mathrm{Tr}(W\sigma) < 0$ for at least one quantum state σ, which thereby has to be entangled [28, 29]. This can then be used to test for entanglement, in that if W has a negative expectation value with respect to some state, then that state must be entangled. On the other hand, if W has a non-negative expectation value for a state, then this entanglement witness is inconclusive on whether the state is entangled.

In terms of the correlation space described in Section 1.1, if W is written as a linear combination of correlations between some measurements, then it defines a hyperplane in the correlation space as well, with all separable states lying to one side of this hyperplane. It has been shown that the set of all points in correlation space that can be achieved by

separable states forms a convex set, though unlike the case of local realistic models, this set is not a polytope. The existence of entanglement witnesses essentially follows from this point and the geometric Hahn-Banach theorem [28].

An entanglement witness is referred to as optimal if there exists a separable state ρ_{sep} such that $\text{Tr}(W\rho_{\text{sep}}) = 0$. An optimal entanglement witness is essentially one that specifies a hyperplane tangent to the region where the separable states lie, with the set of all optimal entanglement witnesses defining the boundary of this region. Because a state can violate a Bell inequality only if it is entangled, this region must lie inside the classical polytope. Similarly to the case of relative quantum violation of Bell inequalities, the magnitude of a negative expectation value $\text{Tr}(W\sigma) < 0$ for some entanglement witness W and entangled state σ indicates the distance between the entangled state and the hyperplane specified by the entanglement witness, and is thus related to the robustness of the entanglement detection against white noise.

1.2.2 Peres-Horodecki criterion

Another important test for separability is known as the Peres-Horodecki criterion or non-positive partial transpose (NPPT) criterion [30]. This theorem states that for a bipartite separable state $\rho_{\text{sep}} = \sum_{i=1}^{k} p_i \, \rho_i^{(1)} \otimes \rho_i^{(2)}$, if the partial transpose of its density matrix is taken with respect to one subsystem, the resulting operator

$$(\rho_{\text{sep}})^{T_2} = \sum_{i=1}^{k} p_i \, \rho_i^{(1)} \otimes \left(\rho_i^{(2)}\right)^T \tag{1.7}$$

is still a positive operator, where without loss of generality we have taken the partial transpose with respect to the second system. This can be seen by noting that for some bipartite separable state, the subsystem density matrices $\rho_i^{(2)}$ are Hermitian operators with positive eigenvalues. As eigenvalues are preserved when the transpose is taken, their transposes also have real positive eigenvalues, and thus it can be concluded that $(\rho_{\text{sep}})^{T_2}$ is still a positive operator.

By taking the contrapositive of this implication, this is equivalent to the statement that if a bipartite state has a non-positive partial transpose, it must be entangled. The converse statement is also true when the subsystem dimensions are 2×2 or 2×3, but not for any higher dimensions [28]. This essentially arises from the fact that in the 2×2- and 2×3-dimensional cases, any positive map can be decomposed as the sum of a completely positive map and the composition of another completely positive map with the transposition map. Hence if a bipartite state is instead found to have a positive partial transpose, this theorem shows that it must be separable if the dimensions are 2×2 or 2×3, but the test is inconclusive if the dimensions are higher.

1.2.3 Entanglement distillation

For the purposes of some techniques such as the quantum teleportation protocol proposed by Bennett et al. [26], it is assumed at the beginning of the protocol that a pure singlet state is distributed between two parties. However in practical implementations, it may be difficult to distribute a perfect singlet state to the two parties, as some degree of mixing is likely to be introduced by noise in the communication channel. The question then arises as to whether it is still possible to use such states to implement the desired protocol. One approach to this problem, now referred to as entanglement distillation, was studied by Bennett et al. [31]. They considered a situation where the two parties are provided with multiple copies of the state

$$\rho_F = F \left|\Psi_1\right\rangle \left\langle\Psi_1\right| + \frac{1-F}{3} \sum_{\mu=2}^{4} \left|\Psi_\mu\right\rangle \left\langle\Psi_\mu\right|, \tag{1.8}$$

where $|\Psi_\mu\rangle$ with $\mu = 1, 2, 3, 4$ denote the four Bell states. This state is parametrised by F, which gives its fidelity with respect to a pure singlet state, $\langle\Psi_1| \rho_F |\Psi_1\rangle = F$. Bennett et al. showed that given two copies of ρ_F with $F > 1/2$, it is possible to perform local operations and classical communication (LOCC) to obtain, with probability greater than $1/4$, a state $\rho_{F'}$ of the form in Eq. (1.8) with $F' > F$. Local operations refer to operations that each party can carry out on their own qubit without needing access to the other qubit, while classical communication refers to sending information via classical channels.

Given enough copies of such ρ_F, it is hence possible to distil a state of arbitrarily close fidelity to the pure singlet state $|\Psi_1\rangle$. This provides a possible way to cope with noisy quantum channels. The asymptotic number of singlet states that can be distilled from some given state can be used as a measure of entanglement, known as its distillable entanglement. This can be contrasted with another entanglement measure known as the entanglement of formation, which essentially describes the asymptotic number of singlet states required to prepare some given state via LOCC [31]. However, it has been shown that while every bipartite qubit state is distillable [32], in some higher dimensions there exist entangled states that are not distillable [33]. Such states are referred to as bound entangled states, and are examples of states where the entanglement of formation exceeds the distillable entanglement.

We have now discussed some general concepts regarding Bell inequalities and entanglement, and described some of the existing literature concerning their implications and potential applications. In the following chapters, we will proceed to focus more specifically on how the one- and two-body correlations of a quantum state can supply information about these properties. Chapter 2 investigates a Bell inequality recently proposed by Tura et al. [12] which is constructed from such correlations. We study the properties of

this Bell inequality with respect to Dicke states, W states, GHZ states and Smolin states, and compare it to an entanglement witness proposed by Krammer et al. [34] as well as the Werner-Wolf-Żukowski-Brukner inequality [10]. In Chapter 3, we show how we may construct an entanglement witness instead of a Bell inequality from symmetric two-body correlations, and characterise some properties of this entanglement witness. Finally, in Chapter 4 we return to a discussion of some of the entanglement-related properties we have previously highlighted, and consider the Bell inequalities we have investigated in the context of these properties.

Chapter 2

Bell inequalities using one- and two-body correlations

In the previous chapter, we have considered general correlation-based Bell inequalities, as shown in Eq. (1.3). However, not all the correlation terms are necessary to construct a Bell inequality. In particular, in Ref. [12] Tura et al. develop a class of Bell inequalities involving only one- and two-body correlations. Such correlations are more experimentally accessible than higher-order correlations [35], and hence such a Bell inequality may be easier to investigate experimentally. Expressed in the form shown in Eq. (1.3), a Bell inequality constructed from such correlations can be written as

$$\sum_{i=1}^{N} \sum_{a \in \mathcal{M}} \alpha_{ai} \left\langle M_a^{(i)} \right\rangle + \sum_{\substack{i,j=1 \\ i \neq j}}^{N} \sum_{\substack{a,b \in \mathcal{M} \\ a \leq b}} \beta_{ai,bj} \left\langle M_a^{(i)} M_b^{(j)} \right\rangle \leq B_C, \tag{2.1}$$

in other words with all the three-body and higher correlations removed. In particular, the paper investigates Bell inequalities that have only two measurement settings and are symmetric under permutations of the particles. The latter condition implies that the choices of measurement settings are the same across all particles, and that for every fixed a, b, the coefficients α_{ai} and $\beta_{ai,bj}$ with different i, j are all equal. With these restrictions, the general form of the Bell inequality can be simplified to

$$\alpha \left\langle \mathcal{S}_0 \right\rangle + \beta \left\langle \mathcal{S}_1 \right\rangle + \frac{\gamma}{2} \left\langle \mathcal{S}_{00} \right\rangle + \delta \left\langle \mathcal{S}_{01} \right\rangle + \frac{\varepsilon}{2} \left\langle \mathcal{S}_{11} \right\rangle \leq B_C, \tag{2.2}$$

where the symmetric correlation operators are defined as

$$\mathcal{S}_a = \sum_{i=1}^{N} M_a^{(i)}, \quad \mathcal{S}_{ab} = \sum_{\substack{i,j=1 \\ i \neq j}}^{N} M_a^{(i)} M_b^{(j)}. \tag{2.3}$$

For brevity, we shall refer to such a Bell inequality, constructed from symmetric one- and

two-body correlations with two measurement settings, as an S2C2M inequality. A slightly different sign convention has been used here as compared to Ref. [12].

In the case where the measurement settings have only two possible outcomes with values ± 1, the particles can essentially be treated as qubits. Since the two choices of measurement setting must be the same across all particles, they can be parametrised as

$$\begin{aligned} M_0^{(i)} &= \sin\theta_0 \cos\phi_0 \, \sigma_x^{(i)} + \sin\theta_0 \sin\phi_0 \, \sigma_y^{(i)} + \cos\theta_0 \, \sigma_z^{(i)}, \\ M_1^{(i)} &= \sin\theta_1 \cos\phi_1 \, \sigma_x^{(i)} + \sin\theta_1 \sin\phi_1 \, \sigma_y^{(i)} + \cos\theta_1 \, \sigma_z^{(i)}. \end{aligned} \tag{2.4}$$

We note that when $N = 2$, an S2C2M qubit inequality does not reduce exactly to the CHSH inequality, despite the fact that the latter is the only non-trivial Bell inequality for two qubits. This is because an S2C2M inequality requires that the choices of measurements are to be the same across all particles, while the CHSH inequality allows them to be different. In fact, for maximal violation of the CHSH inequality to occur, the possible measurement settings on the two qubits must be different from each other.

Tura et al. focus on the case where $\theta_0 = \phi_0 = \phi_1 = 0$ in Eq. (2.4), leaving only θ_1 as a free parameter, henceforth abbreviated as simply θ. The Bell inequality in Eq. (2.2) can then be expressed concisely as $\langle B(\theta) \rangle \geq 0$, where we define $B(\theta)$ as

$$B(\theta) = B_C \mathbb{I} - \alpha \mathcal{S}_0 - \beta \mathcal{S}_1 - \frac{\gamma}{2} \mathcal{S}_{00} - \delta \mathcal{S}_{01} - \frac{\varepsilon}{2} \mathcal{S}_{11}. \tag{2.5}$$

A negative expectation value $\langle B(\theta) \rangle < 0$ then constitutes a violation of this Bell inequality. This also allows it to serve as an entanglement witness, since a state can violate a Bell inequality only if it is entangled. However, it is not necessarily an optimal entanglement witness, in that there may not exist any separable states that saturate the inequality in Eq. (2.2).

In the following sections, we characterise some properties of S2C2M qubit inequalities by studying several classes of entangled states and determining whether they can violate such inequalities. As a comparison, we also investigate the behaviour of these entangled states with respect to an entanglement witness based on two-body correlations studied by Krammer et al. [34], as well as a Bell inequality based on N-body correlations known as the Werner-Wolf-Żukowski-Brukner (WWZB) inequality [10, 11].

2.1 Entanglement witness using structure factors

In Ref. [34], Krammer et al. developed an entanglement witness based on structure factors. Structure factors are constructed from two-body correlations as well, and can be

measured via scattering experiments. This entanglement witness is defined as

$$W(k) = \mathbb{I} - \frac{1}{2}\left(\bar{\Sigma}(k) + \bar{\Sigma}(-k)\right), \tag{2.6}$$

where $\bar{\Sigma}(k)$ is defined in terms of structure factors,

$$\bar{\Sigma}(k) = \binom{N}{2}^{-1} \left(c_x S_{xx}(k) + c_y S_{yy}(k) + c_z S_{zz}(k)\right), \tag{2.7}$$

with $c_i \in \mathbb{R}$, $|c_i| \leq 1$. The structure factors were defined as

$$S_{\alpha\beta} = \sum_{\substack{i,j=1 \\ i<j}}^{N} e^{ik(r_j - r_i)} \sigma_\alpha^{(i)} \sigma_\beta^{(j)}, \tag{2.8}$$

with the inter-spin distances taken to be normalised to unit length so that $r_j - r_i = j - i$ for all i, j. This operator has positive expectation value on all separable states, and for appropriate choices of $\{c_x, c_y, c_z, k\}$, it can have negative expectation values for some entangled states. This allows it to act as an entanglement witness.

2.2 Werner-Wolf-Żukowski-Brukner inequalities

The Werner-Wolf-Żukowski-Brukner (WWZB) inequalities are an important class of Bell inequalities based on N-body correlations [10, 11]. They involve two choices of measurement settings per qubit,

$$\begin{aligned} M_0^{(i)} &= \sin\theta_0^{(i)} \cos\phi_0^{(i)}\, \sigma_x^{(i)} + \sin\theta_0^{(i)} \sin\phi_0^{(i)}\, \sigma_y^{(i)} + \cos\theta_0^{(i)}\, \sigma_z^{(i)}, \\ M_1^{(i)} &= \sin\theta_1^{(i)} \cos\phi_1^{(i)}\, \sigma_x^{(i)} + \sin\theta_1^{(i)} \sin\phi_1^{(i)}\, \sigma_y^{(i)} + \cos\theta_1^{(i)}\, \sigma_z^{(i)}. \end{aligned} \tag{2.9}$$

This resembles the measurement settings given in Eq. (2.4), but for the WWZB inequality, the values of $\theta_a^{(i)}$ and $\phi_a^{(i)}$ can differ across the qubits, as opposed to the measurement settings used in $B(\theta)$ which are identical for all qubits. In the form described by Żukowski and Brukner [11], the WWZB inequalities can be written as

$$\left| \sum_{s_i=\pm 1} S(s_1, ..., s_N) \sum_{k_i=0,1} s_1^{k_1} ... s_N^{k_N} \left\langle M_{k_1}^{(1)} ... M_{k_N}^{(N)} \right\rangle \right| \leq 2^N, \tag{2.10}$$

where $S(s_1, ..., s_N)$ is any function that takes on only the values ± 1. In the case where $S(s_1, ..., s_N) = \sqrt{2}\cos\left(-\frac{\pi}{4} + (s_1 + ... + s_N - N)\frac{\pi}{4}\right)$, it reproduces the Mermin-Ardehali-Belinskiĭ-Klyshko (MABK) inequalities [7–9]. When $N = 2$, this reduces to the CHSH inequality as well.

We shall focus on the category of WWZB inequalities defined by this choice of function

$S(s_1, ..., s_N)$, and analogously to Eq. (2.5), we define

$$B_W = 2^N \mathbb{I} - \sum_{s_i=\pm 1} S(s_1, ..., s_N) \sum_{k_i=0,1} s_1^{k_1} ... s_N^{k_N} M_{k_1}^{(1)} ... M_{k_N}^{(N)}. \tag{2.11}$$

Again, a negative expectation value $\langle B_W \rangle < 0$ is equivalent to a violation of the WWZB inequality. We also restrict our study to the case where all the $\phi_a^{(i)}$ parameters are set to zero, leaving $2N$ parameters $\left\{\theta_a^{(i)}\right\}$.

2.3 Dicke states

Dicke states are symmetric pure states, defined as

$$\left|D_N^k\right\rangle = s(|N-k, k\rangle),$$

where $|N-k, k\rangle$ denotes a pure product vector of $N-k$ qubits in the $|0\rangle$ state and k qubits in the $|1\rangle$ state, and the function s denotes symmetrization over all particles along with appropriate normalisation. Tura et al. showed [12] that by setting the coefficients in Eqs. (2.2) and (2.5) to be

$$\begin{aligned} \alpha &= -N(N-1)(\lceil N/2 \rceil - N/2), \\ \beta &= \alpha/N, \\ \gamma &= -N(N-1)/2, \\ \delta &= -N/2, \\ \varepsilon &= 1, \end{aligned} \tag{2.12}$$

the classical bound has the value $B_C = N/2(N-1)\lceil N/2 + 1 \rceil$. This choice of coefficients detects Bell violations by the Dicke states $\left|D_N^{\lceil N/2 \rceil}\right\rangle$ and $\left|D_N^{\lfloor N/2 \rfloor}\right\rangle$.

In particular, for $\left|D_N^{\lceil N/2 \rceil}\right\rangle$ the expectation value of the $B(\theta)$ operator has the analytic expression

$$\left\langle D_N^{\lceil N/2 \rceil}\right| B(\theta) \left|D_N^{\lceil N/2 \rceil}\right\rangle = 4\lfloor N/2 \rfloor \sin^2(\theta/2) \left((\lceil N/2 \rceil + 1) \sin^2(\theta/2) + 1 \right). \tag{2.13}$$

This attains a minimum value of $-\lfloor N/2 \rfloor / (\lceil N/2 \rceil + 1)$ at

$$\theta_{\min} = \cos^{-1} \frac{\lceil N/2 \rceil}{\lceil N/2 \rceil + 1}, \tag{2.14}$$

corresponding to the maximal violation of local realism. As for the entanglement witness by Krammer et al., $W(k)$ also has negative expectation values on the Dicke states $\left|D_N^{\lceil N/2 \rceil}\right\rangle$ when $k = 0$, $(c_x, c_y, c_z) = (1, 1, -1)$ are chosen to be the parameter values [34].

Such Dicke states can arise as the ground states of the isotropic Lipkin-Meshkov-Glick (LMG) Hamiltonian [36]

$$H_{LMG} = -\frac{\lambda}{N}\sum_{\substack{i,j=1\\ i<j}}^{N}\left(\sigma_x^{(i)}\sigma_x^{(j)} + \sigma_y^{(i)}\sigma_y^{(j)}\right) + h\sum_{i=1}^{N}\sigma_z^{(i)}, \tag{2.15}$$

which has ground state $\left|D_N^{\lceil N/2\rceil}\right\rangle$ when $\lambda/N \geq h > 0$ [37]. λ represents the strength of the couplings between the particles, while h can represent the strength of a magnetic field. As evidenced from the coupling term in the expression, all N particles are coupled to each other under this Hamiltonian, with equal strength for all couplings. It hence involves long-range interactions rather than nearest-neighbour or next-nearest-neighbour interactions. Originally introduced in nuclear physics as a test model for various approximation methods [36], it has since been used to investigate some properties such as phase transitions [37].

We compare the effects of thermal noise under this Hamiltonian on the expectation values of $B(\theta)$, $W(k)$ and B_W, by plotting their expectation values with respect to the mixed state $\rho_T = e^{-H_{LMG}/k_BT}/Z$. As the temperature tends toward infinity, this approaches the maximally mixed state, on which all the correlations are zero. For simplicity, units are chosen such that $k_B = 1$. The coupling constant and magnetic field were set to be $\lambda = 10$ and $h = 0.1$ respectively.

To compare the entanglement witnesses, we need to normalise them to some common standard. We choose to normalise them such that as the temperature goes to infinity and the correlations go to zero, the expectation values of the operators go to 1. We see from Eqs. (2.5), (2.6) and (2.11) that when all correlations go to zero, we have $\langle B(\theta)\rangle = B_C$, $\langle W(k)\rangle = 1$ and $\langle B_W\rangle = 2^N$. Hence in the following analysis, we compare $\langle B(\theta)\rangle / B_C$, $\langle W(k)\rangle$ and $\langle B_W\rangle / 2^N$. This choice of normalisation also gives the relative quantum violation of the Bell inequalities; namely, when the value of $\langle B(\theta)\rangle / B_C$ or $\langle B_W\rangle / 2^N$ is negative, the relative quantum violation is simply the magnitude of this negative value.

For $\langle B(\theta)\rangle / B_C$ and $\langle W(k)\rangle$, if the coefficients $\{\alpha, \beta, \gamma, \delta, \varepsilon\}$ and $\{c_x, c_y, c_z\}$ are fixed as described previously, there remains one free parameter θ and k respectively. Shown in Fig. 2.1 is an example of $\langle B(\theta)\rangle / B_C$ plotted as a function of θ and T, as well as $\langle W(k)\rangle$ plotted as a function of k and T. The graphs suggest that even when the thermal state is not at zero temperature, the most negative value still occurs at $\theta_{\min} = \cos^{-1}(\lceil N/2\rceil/(\lceil N/2\rceil + 1))$ and $k = 0$ respectively, the parameter values which minimise the expectation value for the ground state $\left|D_N^{\lceil N/2\rceil}\right\rangle$. Therefore, in the subsequent analysis, $\langle B(\theta)\rangle / B_C$ and $\langle W(k)\rangle$ are considered at these values of θ and k respectively.

Fig. 2.2 shows the values of $\langle B(\theta_{\min})\rangle / B_C$, $\langle W(0)\rangle$ and $\langle B_W\rangle$ on the thermal state ρ_T as a function of temperature. The values for $\langle B_W\rangle$ were obtained by minimising over the $2N$ angular parameters $\left\{\theta_a^{(i)}\right\}$. In all cases, the most negative value occurs at $T = 0$,

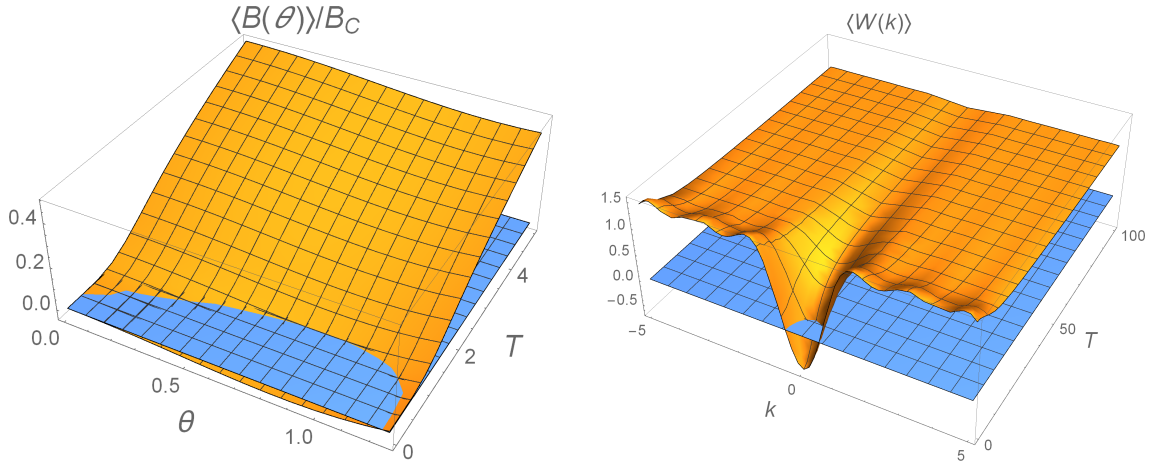

Figure 2.1: Comparison of $\langle B(\theta)\rangle/B_C$ and $\langle W(k)\rangle$ for the four-qubit Dicke state $|D_4^2\rangle$. One horizontal axis on each plot indicates the temperature T, while the other indicates θ and k respectively. Planes are plotted in blue at $\langle B(\theta)\rangle/B_C = 0$, $\langle W(k)\rangle = 0$ to more clearly show which regions are negative. Note that the temperature scales on the two graphs are different, due to the substantially higher robustness of $\langle W(k)\rangle$ against temperature increase. It can be seen that both graphs have regions where the expectation values are negative, but $\langle W(k)\rangle$ remains negative up to higher temperatures than $\langle B(\theta)\rangle/B_C$.

and increases towards 1 as the temperature is increased, as expected. Another quantity of interest that can be obtained from these graphs is the critical temperature T_c at which the expectation value becomes non-negative. These values are summarised in Table 2.1. We note that the critical temperatures are independent of the choice of normalisation, as they only depend on the sign of the expectation values.

Several trends can be noted from the values in Table 2.1. Firstly, the most negative minimum value was attained by $\langle B_W\rangle/2^N$ in all cases other than $N = 3$, followed by $\langle W(0)\rangle$, with $\langle B(\theta_{\min})\rangle/B_C$ being the least negative. Also, the minimum value of $\langle B_W\rangle/2^N$ becomes increasingly negative as N increases, while that of $\langle W(0)\rangle$ and $\langle B(\theta_{\min})\rangle/B_C$ instead decreases in magnitude. This is consistent with the fact that the maximum quantum violation of the WWZB inequality increases exponentially with N for specific states. Recalling that the magnitude of the negative expectation value corresponds to a measure of robustness against white noise as described in Section 1.1, these results indicate that out of these three cases, violation of the WWZB inequality by the ground state $\left|D_N^{\lceil N/2\rceil}\right\rangle$ is the most robust against white noise.

It can also be seen that for any N, $\langle W(0)\rangle$ is the most robust against thermal noise, in the sense of having the highest critical temperature. It is followed by $\langle B_W\rangle/2^N$, then $\langle B(\theta_{\min})\rangle/B_C$. There also appears to be a general decreasing trend in the critical temperatures as N increases. For $\langle B_W\rangle/2^N$ and $\langle B(\theta_{\min})\rangle/B_C$ however, there is a noticeable difference between the even-N and odd-N cases. The even-N cases appear to be more robust against thermal noise as compared to the odd-N cases, with critical temperatures approximately ten times higher. This could be due to the fact that the ground state of the

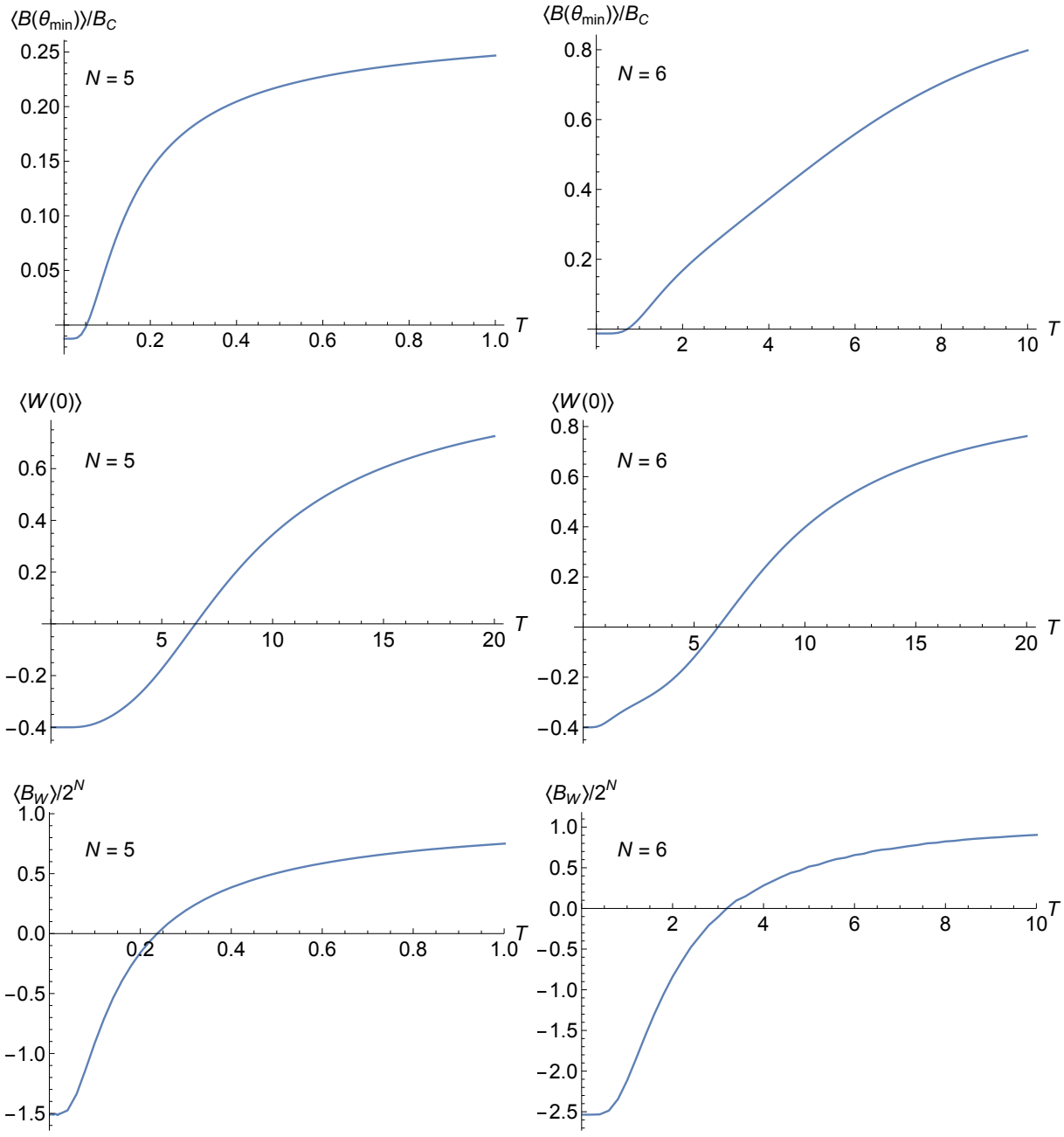

Figure 2.2: Comparison of the effects of temperature on $\langle B(\theta_{\min})\rangle/B_C$, $\langle W(0)\rangle$ and $\langle B_W\rangle/2^N$ for Dicke states $\left|D_N^{\lceil N/2\rceil}\right\rangle$ with $N = 5, 6$. These expectation values increase as the temperature T increases, starting from some negative value and approaching 1 at high temperatures. Noting that the scales on the graphs are different, it can be seen that the critical temperatures where the value becomes positive are lower for $\langle B(\theta_{\min})\rangle/B_C$ as compared to $\langle W(0)\rangle$ and $\langle B_W\rangle/2^N$. In addition, there is a substantial difference between the $N = 5$ (odd) and $N = 6$ (even) cases for $\langle B(\theta_{\min})\rangle/B_C$ and $\langle B_W\rangle/2^N$, which can be seen in more detail in Table 2.1. It can also be seen that in these graphs, the most negative values are obtained at zero temperature by $\langle B_W\rangle/2^N$.

Table 2.1: Minimum values and critical temperatures for $\langle B(\theta_{\min})\rangle/B_C$, $\langle W(0)\rangle$ and $\langle B_W\rangle/2^N$ with varying N. The critical temperature T_c refers to the temperature at which the expectation value becomes positive. It can be seen that while the magnitudes of the minimum values for $\langle B(\theta_{\min})\rangle/B_C$ and $\langle W(0)\rangle$ are decreasing with N, it instead increases with N for $\langle B_W\rangle/2^N$. As for the critical temperatures, there is a general decreasing trend for larger N, though for $\langle B(\theta_{\min})\rangle/B_C$ and $\langle B_W\rangle/2^N$ there is a clear difference between the cases of odd and even N.

$\langle B(\theta_{\min})\rangle/B_C$		
N	Minimum	T_c
3	$-1/27$	0.07
4	$-1/27$	1.28
5	$-1/80$	0.05
6	$-1/80$	0.72
7	$-1/175$	0.05
8	$-1/175$	0.48

$\langle W(0)\rangle$		
N	Minimum	T_c
3	$-2/3$	8.48
4	$-2/3$	7.21
5	$-2/5$	6.52
6	$-2/5$	6.08
7	$-2/7$	5.79
8	$-2/7$	5.57

$\langle B_W\rangle/2^N$		
N	Minimum	T_c
3	-0.52	0.13
4	-1.12	3.47
5	-1.51	0.24
6	-2.53	3.20
7	-3.38	0.43
8	-5.19	3.15

LMG Hamiltonian is near-degenerate when N is odd, because the $\left|D_N^{\lceil N/2\rceil}\right\rangle$ and $\left|D_N^{\lfloor N/2\rfloor}\right\rangle$ states have an energy separation of only $2h$. Therefore, mixing of the ground state with the first excited state as temperature is increased may occur more rapidly when N is odd.

However, there does not appear to be a similar trend for $\langle W(0)\rangle$, so this may not be the only factor involved. Perhaps another relevant point is the fact that for the choice of coefficients specified in Eq. (2.12), the one-body coefficients α and β are non-zero only when N is odd. This may arise from or lead to different behaviour for the even-N and odd-N cases. In the case of $\langle B_W\rangle/2^N$, it can also be noted that the critical temperature appears to decrease with N when N is odd, yet increase with N when N is even. These trends noted for the WWZB inequality may possibly reflect some known differences in its properties between even and odd N [11, 38].

Overall, $\langle B_W\rangle/2^N$ appears to be the most robust against white noise, while $\langle W(0)\rangle$ is the most robust against thermal noise. $\langle B(\theta_{\min})\rangle/B_C$ is the least robust against both thermal noise and white noise. To some extent, its low robustness as compared to $\langle W(0)\rangle$ may arise from the fact that referring back to Eq. (2.2), we note it was constructed as a Bell inequality rather than an optimal entanglement witness, and hence may lie some distance away from the set of separable states. In Chapter 3, we develop an entanglement witness based on symmetric two-body correlations that is optimal when N is even.

2.4 W states

The W states $|W_N\rangle$ are a subset of the Dicke states, namely those of the form

$$|W_N\rangle = \left|D_N^1\right\rangle = \frac{1}{\sqrt{N}}\left(|10...0\rangle + |01...0\rangle + ... + |00...1\rangle\right). \tag{2.16}$$

They possess entanglement that is robust against particle loss when N is large, in that tracing out any one particle from the state results in a state of the form

$$\rho_{N-1} = \frac{N-1}{N} |W_{N-1}\rangle \langle W_{N-1}| + \frac{1}{N} |00...0\rangle \langle 00...0| , \tag{2.17}$$

which for large N simply approaches the W state with one less particle, $|W_{N-1}\rangle$. In the case $N = 3$, the W state is equivalent to the $\left|D_N^{\lceil N/2 \rceil}\right\rangle$ state considered in Section 2.3, up to unitary rotations. For larger numbers of particles, however, the W states are not equivalent to the $\left|D_N^{\lceil N/2 \rceil}\right\rangle$ states.

We study the expectation values of $B(\theta)$, $W(k)$ and B_W with respect to W states of $N = 3$ to $N = 6$ particles to determine if W state entanglement can be detected by these operators. The authors of the references describing these Bell inequalities and entanglement witnesses do not give the optimal parameters for these operators to be applied to W states [11, 12, 34], so in each case we numerically minimise the expectation value over the various parameters of the operators. $\langle B(\theta)\rangle$ is minimised over $\{\alpha, \beta, \gamma, \delta, \epsilon, \theta\}$, $\langle W(k)\rangle$ is minimised over $\{c_x, c_y, c_z, k\}$, and $\langle B_W\rangle$ is minimised over the set of $2N$ angles $\left\{\theta_a^{(i)}\right\}$.

For the $|W_3\rangle$ state, both $\langle B(\theta)\rangle$ and $\langle W(k)\rangle$ can indeed be negative, with the same minimum values of $-1/27$ and $-2/3$ as found in Section 2.3. This is as expected from the fact that $|W_N\rangle$ is essentially equivalent to the $\left|D_N^{\lceil N/2 \rceil}\right\rangle$ state when $N = 3$. For $N \geq 4$ however, the numerically-obtained minimum values of $\langle B(\theta)\rangle$ and $\langle W(k)\rangle$ were instead found to be non-negative, suggesting that the entanglement of such W states cannot violate S2C2M inequalities of the form described by $B(\theta)$, or be detected by $W(k)$.

However, $B(\theta)$ does not describe the most general form of S2C2M qubit inequality, as it is subject to the constraints $\theta_0 = \phi_0 = \phi_1 = 0$ in the measurement settings shown in Eq. (2.4). By allowing these parameters to be nonzero, the minimum value of $\langle B(\theta_0, \phi_0, \theta_1, \phi_1)\rangle$ was found to be negative in the $N \geq 4$ cases as well, indicating a violation of the inequality. Similarly, the minimum value of $\langle B_W\rangle$ was also found to be negative for W states. The results are summarised in Fig. 2.3.

It can be seen from the figure that as the number of particles increases, the relative violation of the S2C2M inequality described by $B(\theta_0, \phi_0, \theta_1, \phi_1)$ is decreasing, similar to the trend found for the $\left|D_N^{\lceil N/2 \rceil}\right\rangle$ Dicke states in the previous section. This trend is consistent with the findings by Tura et al. that for the choice of coefficients given in Eq. (2.12), the relative quantum violation of the S2C2M inequality by $\left|D_N^{\lceil N/2 \rceil}\right\rangle$ Dicke states decreases with N. However, we note that Tura et al. also found that for specific choices of coefficients and quantum states, the maximum possible relative violation of S2C2M inequalities can in fact increase with N instead [12]. Our results hence indicate that the trend for W states is similar to that of the $\left|D_N^{\lceil N/2 \rceil}\right\rangle$ Dicke states, rather than the states which give the maximal relative violation of S2C2M inequalities.

As for the relative violation of the WWZB inequality, it can be seen that it still

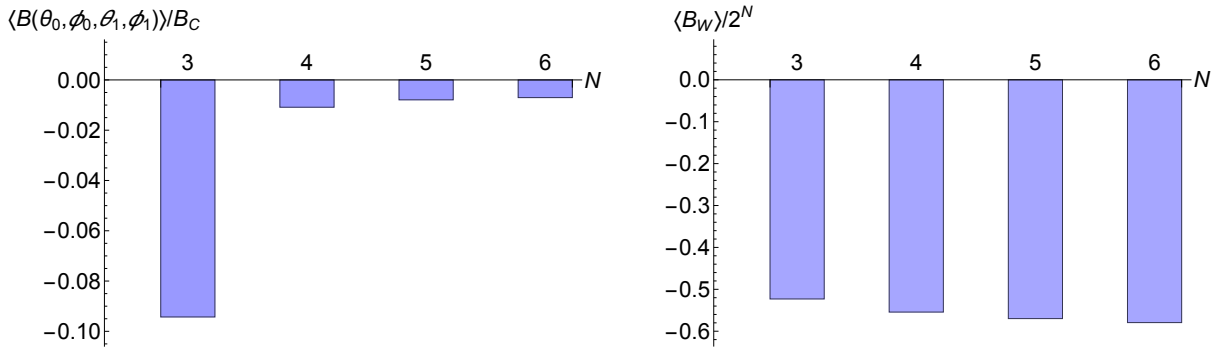

Figure 2.3: Values of $\langle B(\theta_0, \phi_0, \theta_1, \phi_1)\rangle / B_C$ and $\langle W_Z\rangle / 2^N$ for various values of N, corresponding to the relative violations of the inequalities. It appears that the relative violation of the former is decreasing with N, while the latter increases slowly with N.

increases with N, which is somewhat similar to the trend found for the $\left|D_N^{\lceil N/2\rceil}\right\rangle$ Dicke states. However, it differs in that the increase appears to be quite slow, which is also in contrast to the fact that the maximal relative violation of the WWZB inequality increases exponentially with N. Overall, these results suggest that for the Bell inequalities or entanglement witnesses studied in this section, the entanglement of W states is relatively difficult to detect and does not scale well with N. In particular, it seems to be difficult to detect using only two-body correlations, though not impossible as shown by the small negative values of $\langle B(\theta_0, \phi_0, \theta_1, \phi_1)\rangle$.

2.5 Greenberger-Horne-Zeilinger states

Greenberger-Horne-Zeilinger (GHZ) states are states of the form

$$|GHZ\rangle = \frac{1}{\sqrt{2}}\left(|0\rangle^{\otimes N} + |1\rangle^{\otimes N}\right).$$

They possess a number of interesting entanglement properties, and maximally violate certain classes of Bell inequalities [11, 38, 39]. However, we shall now show that it is not possible for GHZ states with $N > 2$ to violate any Bell inequality constructed from one- and two-body correlations. Physically, this arises from the fact that tracing out any number of particles from the GHZ state results in states that are indistinguishable from those obtained by tracing out particles from the state $\rho = \frac{1}{2}\left(\left(|0\rangle\langle 0|\right)^{\otimes N} + \left(|1\rangle\langle 1|\right)^{\otimes N}\right)$, which is separable.

2.5.1 Two-body correlations

We first consider an N-qubit Bell inequality involving only two-body correlations, with two measurement settings $M_0^{(i)} = \cos\theta_0^{(i)}\,\sigma_z^{(i)} + \sin\theta_0^{(i)}\,\sigma_x^{(i)}$ and $M_1^{(i)} = \cos\theta_1^{(i)}\,\sigma_z^{(i)} + \sin\theta_1^{(i)}\,\sigma_x^{(i)}$ for each qubit. Using the notation of Eq. (2.1), such a Bell inequality can be expressed

in the form

$$\sum_{\substack{i,j=1\\ i\neq j}}^{N} \sum_{a,b\in\{0,1\}} \beta_{ai,bj} \left\langle M_a^{(i)} M_b^{(j)} \right\rangle \leq B_C. \tag{2.18}$$

As described in Section 1.1, the classical bound can be found by taking the largest value over the vertices of the classical polytope, namely the deterministic local realistic models such that $\left\langle M_a^{(i)} M_b^{(j)} \right\rangle = \left\langle M_a^{(i)} \right\rangle \left\langle M_b^{(j)} \right\rangle$ with $\left\langle M_a^{(i)} \right\rangle = \pm 1$. For brevity, we shall subsequently refer to such an assignment of values as a "vertex strategy". We then have

$$B_C = \max \left\{ \sum_{\substack{i,j=1\\ i\neq j}}^{N} \sum_{a,b\in\{0,1\}} \beta_{ai,bj} \left\langle M_a^{(i)} \right\rangle \left\langle M_b^{(j)} \right\rangle \middle| \left\langle M_a^{(i)} \right\rangle = \pm 1 \right\}. \tag{2.19}$$

We now consider an N-qubit GHZ state with $N > 2$. By viewing $\sigma_x^{(i)}$ as a bit-flip on the i^{th} site, it can be seen that for $N > 2$ and $i \neq j$, we always have $\langle GHZ| \sigma_x^{(i)} \sigma_z^{(j)} |GHZ\rangle = 0$ and $\langle GHZ| \sigma_x^{(i)} \sigma_x^{(j)} |GHZ\rangle = 0$. Therefore,

$$\begin{aligned} \langle GHZ| M_a^{(i)} M_b^{(j)} |GHZ\rangle &= \langle GHZ| \cos\theta_a^{(i)} \cos\theta_b^{(j)} \sigma_z^{(i)} \sigma_z^{(j)} |GHZ\rangle \\ &= \cos\theta_a^{(i)} \cos\theta_b^{(j)}. \end{aligned} \tag{2.20}$$

Hence for a GHZ state, the left-hand side of Eq. (2.18) simplifies to the following expression, which we shall denote as Q_{GHZ}:

$$Q_{\text{GHZ}} = \sum_{\substack{i,j=1\\ i\neq j}}^{N} \sum_{a,b\in\{0,1\}} \beta_{ai,bj} C_{ia} C_{jb}, \tag{2.21}$$

where $C_{ia} = \cos\theta_a^{(i)} \in [-1, 1]$. The form of this expression is very similar to the values taken at the vertices of the classical polytope, except that the $\{C_{ai}\}$ can take values in the whole interval $[-1, 1]$ rather than only the extremal values ± 1. We shall now show that Q_{GHZ} can never exceed the classical bound B_C given by maximising over the vertices of the classical polytope, and hence the GHZ state cannot violate such a Bell inequality.

We first consider the case where none of the coefficients $\{\beta_{ai,bj}\}$ are zero. It suffices to show that Q_{GHZ} in Eq. (2.21) attains its maximum when the values of $\{C_{ia}\}$ are extremal, since this corresponds to a value at one of the vertices of the classical polytope and the classical bound is the maximum of all such values.

Suppose to the contrary that Q_{GHZ} is maximised when at least one of the C_{ia}, henceforth denoted as x, is not extremal. Looking at the form of the expression, because the summation excludes all terms with $i = j$, it can be seen to be linear with respect to x.

Since it is linear and x is not extremal, the value of Q_{GHZ} can be further increased by either increasing or decreasing the value of x, contradicting the hypothesis that Q_{GHZ} was already maximal. Hence by contradiction, Q_{GHZ} can only attain its maximum when the values of $\{C_{ia}\}$ are extremal.

For the case where some of the $\{\beta_{ai,bj}\}$ are zero, we have to consider the possibility that the $\{\beta_{ai,bj}\}$ with value zero are such that all terms involving some of the C_{ia}'s are eliminated from the expression. However, a similar argument can still be applied simply by setting the values of such C_{ia} to arbitrary extremal values, since Q_{GHZ} is independent of the values of these C_{ia} in such a case. We have thus shown that the GHZ state with $N > 2$ particles cannot violate Bell inequalities constructed from only two-body correlations.

2.5.2 One- and two-body correlations

Using the result from the previous section, we can now also consider Bell inequalities involving both one- and two-body correlations, the general form shown in Eq. (2.1). We first note that for the GHZ state, $\langle GHZ|\, \sigma_x^{(i)}\, |GHZ\rangle = 0$ holds for similar reasons as in the previous section. In addition,

$$\begin{aligned}\langle GHZ|\, \sigma_z^{(i)}\, |GHZ\rangle &= \frac{1}{2}\left(\langle 00...0| + \langle 11...1|\right)\left(|00...0\rangle - |11...1\rangle\right) \\ &= 0. \end{aligned} \tag{2.22}$$

Therefore, the one-body correlations $\langle GHZ|\, M_a^{(i)}\, |GHZ\rangle$ are all zero. Hence for the GHZ state, the vector of one- and two-body correlations has entries

$$\begin{aligned}&\left(\left\langle M_0^{(1)}\right\rangle, \left\langle M_1^{(1)}\right\rangle, ..., \left\langle M_0^{(1)} M_0^{(2)}\right\rangle, \left\langle M_0^{(1)} M_1^{(2)}\right\rangle, ...\right)_{GHZ} \\ &\qquad = \left(0, 0, ..., C_{01}C_{02}, C_{01}C_{12}, ...\right), \end{aligned} \tag{2.23}$$

where $C_{ai} \in [-1, 1]$ as before.

From the result of the previous section, we know that the vector of two-body correlations for the GHZ state lies within the classical polytope, and can hence be expressed as a convex combination of the vertices,

$$\left(C_{01}C_{02}, C_{01}C_{12}, ...\right) = \sum_k p_k \left(V_{01k}V_{02k}, V_{01k}V_{12k}, ...\right) \tag{2.24}$$

for some set of non-negative p_k summing to 1 with $V_{aik} = \pm 1$ being the vertex strategies. We now note that for each vertex P of the classical polytope, there is a corresponding vertex P' in which all the one-body correlations have the opposite sign from P but all the two-body correlations are the same as P. This is obtained simply by flipping all signs in the vertex strategy corresponding to P, which causes the one-body correlations to change

sign while the sign changes cancel on the two-body correlations. The vector of one- and two-body correlations for the GHZ state can thus also be written as a convex combination of the vertices of the classical polytope by using the same set of p_k as in the decomposition of the vector of two-body correlations,

$$(0, 0, 0, ..., C_{01}C_{02}, C_{01}C_{12}, ...) = \sum_k \frac{p_k}{2} \left(P_k + P'_k\right), \tag{2.25}$$

since the one-body correlations for P_k and P'_k have opposite sign and cancel each other out. This hence shows that the vector of one- and two-body correlations for the GHZ state also lies within the classical polytope, i.e. the GHZ state cannot violate such a Bell inequality either.

The argument is easily generalised to the case where the measurements are allowed to take arbitrary directions, $M_a^{(i)} = \sin\theta_a^{(i)} \cos\phi_a^{(i)} \sigma_x^{(i)} + \sin\theta_a^{(i)} \sin\phi_a^{(i)} \sigma_y^{(i)} + \cos\theta_a^{(i)} \sigma_z^{(i)}$, because $\sigma_y^{(i)}$ behaves similarly to $\sigma_x^{(i)}$ for the purposes of this argument. In addition, it can also be generalised to show that an N-qubit GHZ state cannot violate any Bell inequality constructed using only one- to M-body correlations with $M < N$. This holds because by similar reasoning as before, it can be shown that for the GHZ state, the M-body correlations with odd M all have value 0, while those with even M all take the form $C_{ia}C_{jb}C_{kc}C_{ld}...$ with $C_{ia} \in [-1, 1]$. The argument for two-body correlations can then be used to show it that cannot violate Bell inequalities with any combination of M-body correlations where M is even and less than N, while the argument for one- and two-body correlations completes the proof by showing that it cannot violate Bell inequalities for any combination of one- to M-body correlations with $M < N$.

On the other hand, the reason that a Bell inequality involving N-body correlations can be violated by an N-qubit GHZ state is because for N-body correlations, the terms that are products of all σ_x and σ_y operators can be non-zero, as they flip all the bits in the GHZ state rather than only some of them. This leads to an expression with a different form from those discussed above – for instance, in the two-qubit case it gives the $\cos\left(\theta_a^{(i)} - \theta_b^{(j)}\right)$ terms in the CHSH inequality.

2.6 Smolin state

The Smolin state [40] is a four-particle state of the form

$$\rho_{\text{Smolin}} = \frac{1}{4} \sum_{\mu=1}^{4} \left|\Psi_\mu^{(1,2)}\right\rangle \left\langle\Psi_\mu^{(1,2)}\right| \otimes \left|\Psi_\mu^{(3,4)}\right\rangle \left\langle\Psi_\mu^{(3,4)}\right|, \tag{2.26}$$

where $\left|\Psi_\mu^{(i,j)}\right\rangle$ with $\mu = 1, 2, 3, 4$ refer to the four Bell states with respect to particles i and j. The state is symmetric with respect to any of the particles, though this may not

be immediately apparent from the form in Eq. (2.26). The Smolin state possesses bound entanglement in that despite being an entangled state, it does not allow entanglement to be distilled between any pair of particles unless the other two particles are brought together [40].

However, it turns out that the Smolin state is also unable to violate any S2C2M inequalities, because the expectation values of all its one- and two-body correlations are simply zero. This can be quickly seen from the fact that tracing out all but one or two of the particles from the Smolin state results in a maximally mixed state. More generally, the Smolin state's entanglement cannot be detected by using only one- and two-body correlations, due to a similar line of reasoning as in the beginning of Section 2.5; namely, the set of one- and two-particle reduced states obtained by tracing out from the Smolin state is indistinguishable from that obtained by tracing out from the four-particle maximally mixed state. This may however have some possible implications regarding the types of entanglement that can be detected by S2C2M inequalities, since the Smolin state possesses a specific form of bound entanglement. This is also discussed in Chapter 4.

From the results of this chapter, we see that S2C2M inequalities can be violated by certain quantum states such as $\left|D_N^{\lceil N/2 \rceil}\right\rangle$ Dicke states and W states, but also that there exist important classes of pure entangled states that do not violate these inequalities, such as GHZ states. In addition, the relative quantum violations of the S2C2M inequality tend to be relatively weak compared to entanglement detection by $W(k)$ or violation of the WWZB inequality. However, if we choose to focus on entanglement detection rather than violation of local realism, it may perhaps be possible to construct an entanglement witness using symmetric one- and two-body correlations that detects entanglement more robustly than $B(\theta)$. In the following chapter, we show that this is indeed possible, and investigate some properties of the entanglement witness we derive.

Chapter 3

Entanglement witness using two-body correlations

As previously discussed, the entanglement witness defined by Eq. (2.5) may not be optimal, because it is not known whether the inequality can be saturated by any separable state. This arises from the fact that it was initially constructed to be a Bell inequality rather than an entanglement witness. We now construct an entanglement witness using the symmetric two-body correlation terms in Eqs. (2.2) and (2.5), which lies closer to the set of separable states than the classical bound in an S2C2M inequality. For the case where N is even, the entanglement witness thus constructed is in fact optimal.

3.1 Construction of entanglement witness

Such an entanglement witness can be constructed by finding the maximum of the expression on the left-hand side of Eq. (2.2) over all separable states instead of over all vertices of the classical polytope. Essentially, if a function F can be found such that

$$\frac{\gamma}{2}\langle \mathcal{S}_{00}\rangle + \delta\langle \mathcal{S}_{01}\rangle + \frac{\varepsilon}{2}\langle \mathcal{S}_{11}\rangle \leq F(\gamma,\delta,\varepsilon,\theta) \tag{3.1}$$

for all separable states, then we can construct an entanglement witness

$$A(\theta) = \mathbb{I} - \frac{\frac{\gamma}{2}\mathcal{S}_{00} - \delta\mathcal{S}_{01} - \frac{\varepsilon}{2}\mathcal{S}_{11}}{F(\gamma,\delta,\varepsilon,\theta)}, \tag{3.2}$$

since the expectation value of this operator is positive for all separable states. This expression is chosen such that its expectation value is 1 for the maximally mixed state, matching the choice of normalisation convention used in earlier sections. Again, such a normalisation convention implies that the magnitude of a negative expectation value gives the relative quantum violation of the bound $F(\gamma,\delta,\varepsilon,\theta)$ and corresponds to robustness against white noise. The entanglement witness is optimal if the inequality in Eq. (3.1) is

saturated by some separable state, which occurs if $F(\gamma, \delta, \varepsilon, \theta)$ is precisely the maximum of the left-hand side over all separable states.

We begin by noting that it suffices to find the maximum of the expression for all pure separable states, rather than having to consider mixed separable states as well. This is because as previously stated regarding Eq. (1.6), any separable mixed state ρ_{sep} can be written as a convex combination of product states such that all the subsystem states $\rho_i^{(j)}$ are pure. Hence if the inequality in Eq. (3.1) is satisfied for all pure separable states, then any mixed separable state ρ_{sep} also satisfies the inequality, since

$$\begin{aligned}
\left\langle \frac{\gamma}{2}\mathcal{S}_{00} + \delta\mathcal{S}_{01} + \frac{\varepsilon}{2}\mathcal{S}_{11} \right\rangle_{\rho_{\text{sep}}} &= \text{Tr}\left(\left(\frac{\gamma}{2}\mathcal{S}_{00} + \delta\mathcal{S}_{01} + \frac{\varepsilon}{2}\mathcal{S}_{11} \right) \rho_{\text{sep}} \right) \\
&= \text{Tr}\left(\left(\frac{\gamma}{2}\mathcal{S}_{00} + \delta\mathcal{S}_{01} + \frac{\varepsilon}{2}\mathcal{S}_{11} \right) \sum_{i=1}^{m} p_i \, \rho_i^{(1)} \otimes \rho_i^{(2)} \otimes ... \otimes \rho_i^{(N)} \right) \\
&= \sum_{i=1}^{m} p_i \, \text{Tr}\left(\left(\frac{\gamma}{2}\mathcal{S}_{00} + \delta\mathcal{S}_{01} + \frac{\varepsilon}{2}\mathcal{S}_{11} \right) \rho_i^{(1)} \otimes \rho_i^{(2)} \otimes ... \otimes \rho_i^{(N)} \right) \\
&\leq \sum_{i=1}^{m} p_i \, F(\gamma, \delta, \varepsilon, \theta), \text{ by choosing all } \rho_i^{(j)} \text{ to be pure} \\
&= F(\gamma, \delta, \varepsilon, \theta). \qquad (3.3)
\end{aligned}$$

For a pure separable state $\rho_{\text{sep}} = \rho^{(1)} \otimes \rho^{(2)} \otimes ... \otimes \rho^{(N)}$, the state $\rho^{(i)}$ of each qubit is characterised by a Bloch vector $\hat{n}_i$ of norm 1,

$$\rho^{(i)} = \frac{\mathbb{I} + \hat{n}_i \cdot \vec{\sigma}}{2}, \qquad (3.4)$$

where $\vec{\sigma}$ is the Pauli vector $(\sigma_x, \sigma_y, \sigma_z)$. Using the fact that $\langle \vec{\sigma} \rangle_{\rho^{(i)}} = \hat{n}_i$, the expectation values of the symmetric two-body correlations can be expressed in terms of the Bloch vector components $\hat{n}_i = (x_i, y_i, z_i)$:

$$\langle \mathcal{S}_{00} \rangle = \sum_{\substack{i,j=1 \\ i \neq j}}^{N} \langle \sigma_z^{(i)} \sigma_z^{(j)} \rangle = \sum_{\substack{i,j=1 \\ i \neq j}}^{N} z_i z_j, \qquad (3.5)$$

$$\langle \mathcal{S}_{01} \rangle = \sum_{\substack{i,j=1 \\ i \neq j}}^{N} \langle \sigma_z^{(i)} \left(\sin\theta \, \sigma_x^{(j)} + \cos\theta \, \sigma_z^{(j)} \right) \rangle = \sum_{\substack{i,j=1 \\ i \neq j}}^{N} \left(\sin\theta \, z_i x_j + \cos\theta \, z_i z_j \right), \qquad (3.6)$$

$$\langle \mathcal{S}_{11} \rangle = \sum_{\substack{i,j=1 \\ i \neq j}}^{N} \left(\sin^2\theta \, x_i x_j + \cos^2\theta \, z_i z_j + 2\cos\theta \sin\theta \, z_i x_j \right), \qquad (3.7)$$

using the measurement settings given in Eqs. (2.4) with $\theta_0 = \phi_0 = \phi_1 = 0$ and $\theta_1 = \theta$. The third expression was simplified slightly by noting that $\sum_{i,j} x_i z_j = \sum_{i,j} z_i x_j$.

In addition, we note that

$$\sum_{\substack{i,j=1\\ i\neq j}}^{N} z_i z_j = \left(\sum_{i=1}^{N} z_i\right)\left(\sum_{j=1}^{N} z_j\right) - \sum_{i=1}^{N} z_i^2 = N^2\overline{z}^2 - N\overline{z^2}, \tag{3.8}$$

where we introduce the notation $\overline{f(z)} = \frac{1}{N}\sum_{i=1}^{N} f(z_i)$ for any function f. Essentially, this is an average over the Bloch components of the individual qubits. A similar result holds for $\overline{x}$ and $\overline{x^2}$, as well as $\overline{z}\,\overline{x}$ and $\overline{zx}$. Combining these results, we find that

$$\begin{aligned}\left\langle \frac{\gamma}{2}\mathcal{S}_{00} + \delta\mathcal{S}_{01} + \frac{\varepsilon}{2}\mathcal{S}_{11}\right\rangle &= \sum_{\substack{i,j=1\\ i\neq j}}^{N} \left(A_{zz} z_i z_j + A_{zx} z_i x_j + A_{xx} x_i x_j\right) \\ &= N^2\left(A_{zz}\overline{z}^2 + A_{zx}\overline{z}\,\overline{x} + A_{xx}\overline{x}^2\right) - N\left(A_{zz}\overline{z^2} + A_{zx}\overline{zx} + A_{xx}\overline{x^2}\right),\end{aligned} \tag{3.9}$$

where $A_{zz} = \frac{\gamma}{2} + \delta\cos\theta + \frac{\varepsilon}{2}\cos^2\theta$, $A_{zx} = \delta\sin\theta + \varepsilon\sin\theta\cos\theta$, $A_{xx} = \frac{\varepsilon}{2}\sin^2\theta$ have been introduced for conciseness.

We now make use of the fact that any quadratic form can be diagonalised with an orthogonal transformation $(z\ x)^T = M(z'\ x')^T$ where M is a 2×2 orthogonal matrix, yielding

$$A_{zz}z^2 + A_{zx}zx + A_{xx}x^2 = \lambda_z z'^2 + \lambda_x x'^2, \tag{3.10}$$

with λ_z, λ_x given by

$$\begin{aligned}\lambda_z &= \frac{1}{2}\left(A_{zz} + A_{xx} - \sqrt{A_{zz}^2 + A_{zx}^2 + A_{xx}^2 - 2A_{zz}A_{xx}}\right), \\ \lambda_x &= \frac{1}{2}\left(A_{zz} + A_{xx} + \sqrt{A_{zz}^2 + A_{zx}^2 + A_{xx}^2 - 2A_{zz}A_{xx}}\right).\end{aligned} \tag{3.11}$$

Hence by introducing a change of coordinates $(z_i\ x_i)^T = M(z_i'\ x_i')^T$ on the individual Bloch vectors, it can be shown that

$$A_{zz}\overline{z^2} + A_{zx}\overline{zx} + A_{xx}\overline{x^2} = \lambda_z\overline{z'^2} + \lambda_x\overline{x'^2}, \tag{3.12}$$

$$A_{zz}\overline{z}^2 + A_{zx}\overline{z}\,\overline{x} + A_{xx}\overline{x}^2 = \lambda_z\overline{z'}^2 + \lambda_x\overline{x'}^2. \tag{3.13}$$

We hence wish to maximise

$$\left\langle \frac{\gamma}{2}\mathcal{S}_{00} + \delta\mathcal{S}_{01} + \frac{\varepsilon}{2}\mathcal{S}_{11}\right\rangle = N^2\left(\lambda_z\overline{z'}^2 + \lambda_x\overline{x'}^2\right) - N\left(\lambda_z\overline{z'^2} + \lambda_x\overline{x'^2}\right), \tag{3.14}$$

subject to the constraints $z_i^2 + x_i^2 \leq 1$. Because the transformation was orthogonal, we have $z_i'^2 + x_i'^2 = z_i^2 + x_i^2$ and thus the constraints can be equivalently stated as $z_i'^2 + x_i'^2 \leq 1$.

Noting that $\overline{z'^2} - \overline{z'}^2$ is essentially the variance of the set $\{z'_i\}$ and thus $\overline{z'^2} - \overline{z'}^2 \geq 0$ with equality if and only if all z'_i have the same value, we see that

$$\begin{aligned} N^2\overline{z'}^2 - N\overline{z'^2} &\leq (N^2 - N)\overline{z'^2}, \\ N^2\overline{z'}^2 - N\overline{z'^2} &\geq -N\overline{z'^2}. \end{aligned} \tag{3.15}$$

The upper bound is achieved if and only if all z'_i have the same value, while the lower bound is achieved if and only if $\overline{z'} = 0$. These bounds can be summarised as stating that for any λ_z, we have $\lambda_z \left(N^2\overline{z'}^2 - N\overline{z'^2} \right) \leq \max\left\{\lambda_z(N^2 - N), -\lambda_z N\right\} \overline{z'^2}$. A similar statement holds for the x' terms, leading to the final bound on Eq. (3.14),

$$\begin{aligned} \left\langle \frac{\gamma}{2}\mathcal{S}_{00} + \delta\mathcal{S}_{01} + \frac{\varepsilon}{2}\mathcal{S}_{11} \right\rangle &= \lambda_z \left(N^2\overline{z'}^2 - N\overline{z'^2} \right) + \lambda_x \left(N^2\overline{x'}^2 - N\overline{x'^2} \right) \\ &\leq \max\left\{\lambda_z(N^2 - N), -\lambda_z N\right\} \overline{z'^2} + \max\left\{\lambda_x(N^2 - N), -\lambda_x N\right\} \overline{x'^2} \\ &\leq \max\left\{\lambda_z(N^2 - N), -\lambda_z N, \lambda_x(N^2 - N), -\lambda_x N\right\}. \end{aligned} \tag{3.16}$$

The last step is achieved by noting that $C_z z_i'^2 + C_x x_i'^2 \leq \max\{C_z, C_x\}$ under the constraint $z_i'^2 + x_i'^2 \leq 1$, which can be proven by Lagrange multipliers or by viewing it as essentially finding the extremal points of an ellipse.

We have thus found that $F(\gamma, \delta, \varepsilon, \theta) = \max\{\lambda_z(N^2 - N), -\lambda_z N, \lambda_x(N^2 - N), -\lambda_x N\}$ is a function that satisfies the condition in Eq. (3.1), and can thus be used to construct an entanglement witness $A(\theta)$ as in Eq. (3.2). When N is even, this bound is optimal, as we now show by explicitly constructing a separable state that saturates this inequality. For the case where the maximum of the quantities in Eq. (3.16) is $\lambda_z(N^2 - N)$, the bound is achieved by the state with $z'_i = 1$, $x'_i = 0$ for all the qubits. This can then be converted back into values for the original Bloch components z_i and x_i by inverting the orthogonal transformation $(z_i \ x_i)^T = M(z'_i \ x'_i)^T$. For the case where the maximum is $-\lambda_z N$, the bound is achieved by the state with $z'_i = 1$, $x'_i = 0$ for half the qubits and $z'_i = -1$, $x'_i = 0$ for the remaining half, yielding $\overline{z'^2} = 1$ and $\overline{z'} = 0$. The cases where the maximum is $\lambda_x(N^2 - N)$ or $-\lambda_x N$ are similar.

If N is odd, the conditions $\overline{z'^2} = 1$ and $\overline{z'} = 0$, or similarly for x', cannot be fulfilled simultaneously, and thus the inequality cannot be saturated for certain combinations of values for λ_z, λ_x. However, we note that for increasing values of odd N, the bound becomes increasingly tight, because when N is large it is possible to approach $\overline{z'^2} \approx 1$ and $\overline{z'} \approx 0$ even when N is odd. This entanglement witness thus becomes closer to optimal for odd N when N is large.

3.2 Characterisation of entanglement witness

The expression in Eq. (3.1), constructed from symmetric two-body correlations with two measurement settings, only has three correlation terms $\langle \mathcal{S}_{00} \rangle$, $\langle \mathcal{S}_{01} \rangle$ and $\langle \mathcal{S}_{11} \rangle$. Therefore, this correlation space effectively has only three dimensions and can be represented graphically on a three-dimensional plot. Some such plots, for the $N = 4$ case, are shown in Fig. 3.1. The region defined by the entanglement witness was plotted approximately by finding the tangent planes specified by the entanglement witness in 50 directions, then displaying the polytope defined by these tangent planes, shown in blue in Fig. 3.1. Due to this plotting method, the blue polytope is not an exact depiction of the true region defined by the entanglement witness. As the blue polytope is constructed by finding a finite number of tangent planes, the true region is strictly contained within the blue polytope, with each facet being tangent to that region at some point. However by finding a sufficiently large number of tangent planes in approximately uniformly distributed directions, it should be a reasonably good depiction. Also shown in the plots is the classical polytope in yellow, obtained by explicitly enumerating the vertices as described in Section 1.1.

Since an even value of N is used in Fig. 3.1, the entanglement witness is optimal and hence precisely demarcates the region in the correlation space where all separable states lie. As stated in Section 1.2.1, this is supposed to be a convex set that is not a polytope, though the plotting method used here creates an approximate depiction of it as the blue polytope instead. Approximate plotting techniques aside, it can be seen from the plots that this region is contained entirely within the classical polytope, as expected. As the value of θ increases from 0 to π, this region moves across the polytope, and it narrows into a line segment for the $\theta = 0$ and $\theta = \pi$ degenerate cases. In contrast, Fig. 3.2 shows an odd-N case, specifically $N = 5$. The non-optimality of the witness $A(\theta)$ can be seen from the fact that the blue region protrudes slightly from the classical polytope. Since the region where the separable states can lie should be contained strictly within the classical polytope, this indicates that the bound is non-optimal for this case.

Fig. 3.3 shows the coordinates in correlation space of the thermal state of the LMG Hamiltonian, $\rho_T = e^{-H_{LMG}/k_B T}/Z$, for $N = 4$. The red dot indicates the ground state $\left| D_N^{\lceil N/2 \rceil} \right\rangle$ and the blue line indicates the location of the thermal state as T increases. Consistent with the results of Section 2.3, the ground state lies outside the classical polytope, indicating that it can violate an S2C2M inequality. The set of coefficients shown in Eq. (2.12) and the corresponding bound $B_C = N/2(N-1)\lceil N/2 + 1 \rceil$ in fact specify precisely the facet of the polytope nearest to the red dot in the figure. As the temperature increases, the thermal state moves into the classical polytope, with the point where it crosses the facet corresponding to the critical temperature T_c. There is a range of temperatures past T_c in which it remains outside the region defined by $A(\theta)$ and hence can still be detected by this entanglement witness despite not violating any S2C2M inequalities.

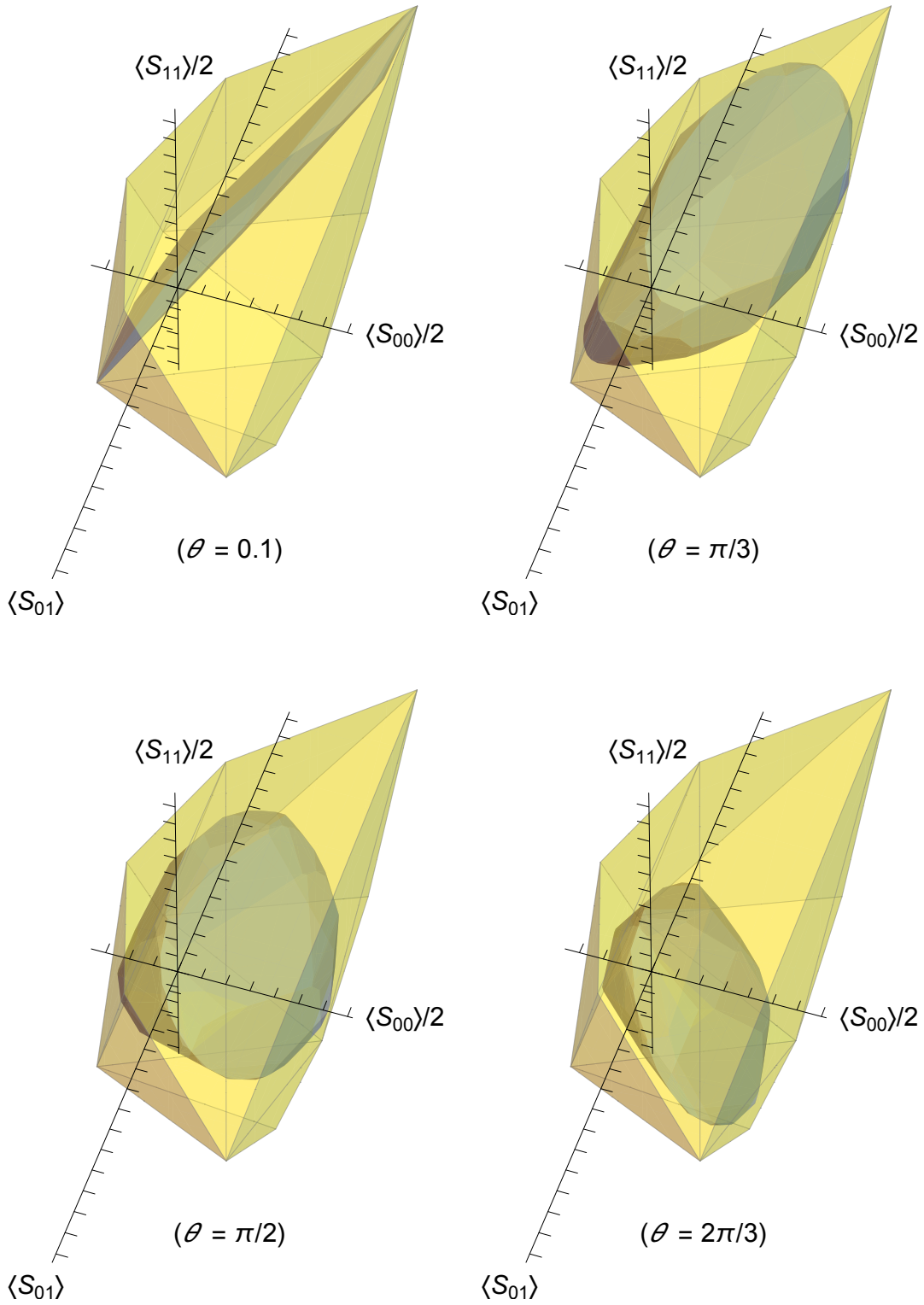

Figure 3.1: Plots of the region in correlation space defined by the entanglement witness $A(\theta)$ for $N = 4$ with various values of θ. The blue region is an approximate depiction of the region defined by $A(\theta)$, while the yellow region shows the classical polytope. To reduce clutter, numerical values have been suppressed on the axes, and instead ticks have been placed at unit intervals. Since the value of N is even, $A(\theta)$ is an optimal entanglement witness for this case, and thus the blue region lies entirely within the classical polytope as expected.

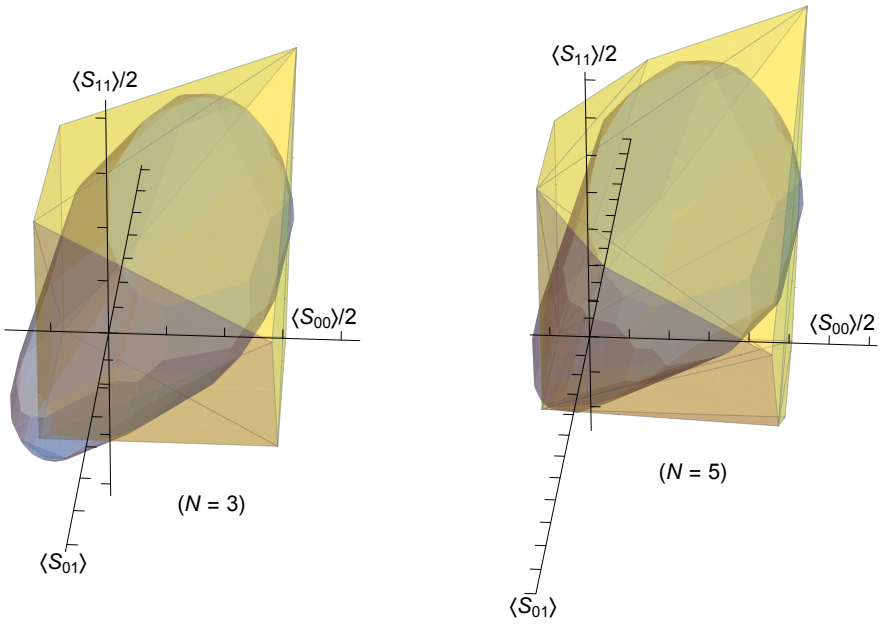

Figure 3.2: Plots of the region in correlation space defined by the entanglement witness $A(\theta)$ for odd values of N with $\theta = \pi/3$. The blue region is an approximate depiction of the region defined by $A(\theta)$, while the yellow region shows the classical polytope. To reduce clutter, numerical values have been suppressed on the axes, and instead ticks have been placed at intervals of 1 for the $N = 3$ case and intervals of 2 for the $N = 5$ case. It can be seen that the blue region exceeds the boundaries of the classical polytope, indicating that the entanglement witness is nonoptimal for these cases.

The magnitude of the relative quantum violation is also larger for $A(\theta)$ than $B(\theta)$, since $A(\theta)$ is an optimal witness for even N and the region it defines lies strictly inside the classical polytope.

Due to the reasons discussed in Sections 2.5 and 2.6, it is not possible to detect the entanglement of GHZ states and Smolin states using the entanglement witness $A(\theta)$. Therefore, we investigated its expectation value for Dicke states of the form $\left|D_N^{\lceil N/2 \rceil}\right\rangle$ as well as W states. It was found that similar to $B(\theta)$ and $W(k)$ discussed in Section 2.4, $A(\theta)$ is also unable to detect the entanglement of W states for $N > 3$, with an expectation value that is always non-negative for such states. Given that $B(\theta_0, \phi_0, \theta_1, \phi_1)$ was able to detect W state entanglement, it may be possible that generalising $A(\theta)$ to allow the other measurement angles θ_0, ϕ_0, ϕ_1 to be nonzero may allow it to detect such entanglement.

As for the $\left|D_N^{\lceil N/2 \rceil}\right\rangle$ Dicke states, $A(\theta)$ was able to detect such entanglement, with negative expectation values that are larger in magnitude than those of the Bell operator $B(\theta)$. The minimum expectation values for such Dicke states are shown in Fig. 3.4. From the figure, it can be seen that for even values of N, the magnitude of the negative expectation value appears to be decreasing, while the opposite trend appears to hold for odd N. This may be a result of the fact that the entanglement witness is not optimal for odd N, and thus the relative quantum violation of the bound $F(\gamma, \delta, \varepsilon, \theta)$ is smaller. The increasing trend for such N may be due to the fact that as described in the previous

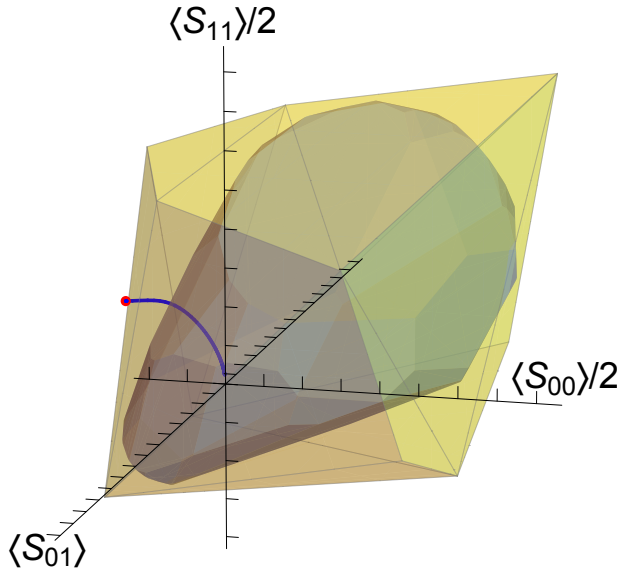

Figure 3.3: Plot of the coordinates in correlation space of the thermal state $\rho_T = e^{-H_{LMG}/k_BT}/Z$ for $N = 4$, along with the region defined by the entanglement witness $A(\theta)$ with $\theta = \cos^{-1}(\lceil N/2 \rceil / (\lceil N/2 \rceil + 1))$ in blue and the classical polytope in yellow. To reduce clutter, numerical values have been suppressed on the axes, and instead ticks have been placed at unit intervals. The red dot denotes the point corresponding to $T = 0$. As the temperature increases, the state's position in correlation space moves towards the origin. It first enters the classical polytope at the critical temperature T_c, then enters the region defined by $A(\theta)$.

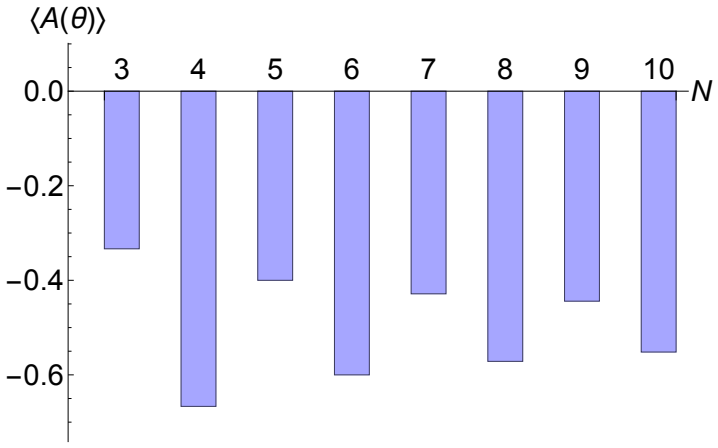

Figure 3.4: Values of $\langle A(\theta) \rangle$ for the $\left| D_N^{\lceil N/2 \rceil} \right\rangle$ Dicke states with various values of N. For even N, the magnitude of the values is decreasing, while for odd N the magnitude is increasing. This may reflect the increasing optimality of the entanglement witness $A(\theta)$ for large odd N, and suggests that the trends may converge as N increases further.

section, the bound $F(\gamma, \delta, \varepsilon, \theta)$ for odd N becomes tighter for large values of N. From the graph, it appears possible that this will cause the trends for odd and even N to converge as N increases, with the overall long-term trend likely being a decrease in magnitude similar to the trend for $B(\theta)$.

Overall, in this chapter we have derived an entanglement witness based on two-body correlations, and shown that it can detect the entanglement of $\left|D_N^{\lceil N/2 \rceil}\right\rangle$ Dicke states. While it is unable to detect W state entanglement, it is possible that a slight generalisation to allow arbitrary measurement directions may allow it to do so. We have also discussed its relation to the classical polytope, as well as its increasing optimality for odd N as N increases. The following chapter returns to S2C2M inequalities and some of the concepts discussed in Chapter 1, discussing how the former may be put into the context of the latter.

Chapter 4

Bell violations, distillability and the Peres-Horodecki criterion

Thus far, we have discussed several properties related to Bell inequalities and entanglement. The necessity or sufficiency of such properties with respect to entanglement are rather complex, with some statements being general while others only apply in specific. In this chapter, we shall discuss how some of these conditions relate to each other, as well as how it may be applied to the results found in previous chapters.

In Chapter 1, it was stated that Bell violation implies entanglement, and that a bipartite state having a non-positive partial transpose implies that it is entangled, but the converses of these statements are not true [28,30]. It is also clear that a state that is distillable has to be entangled, but conversely, it has been shown that there exist entangled states that are not distillable [33]. It is of interest to study the remaining relationships between these properties for bipartite states, which are summarised in Fig. 4.1.

To begin with, a recent result by Vértesi and Brunner showed that there exists a state which violates a Bell inequality but has a positive partial transpose and is not distillable [41], thus Bell violation does not imply either NPPT or distillability. As for the converses of these statements, the two-qubit Werner state $P\left|\Psi\right\rangle\!\left\langle\Psi\right| + (1-P)\,\mathbb{I}/2^N$ where $\left|\Psi\right\rangle$ is the singlet state has a range of values of P for which it is distillable and has non-positive partial transpose, but does not violate any Bell inequality [28,32,42]. Finally, Horodecki et al. showed that any distillable state must satisfy the NPPT criterion [33], while the converse remains an important open question in entanglement theory [41].

This covers all the relationships shown in Fig. 4.1, from which it can be seen that many of these conditions do not imply each other. However, these statements are concerning bipartite states of arbitrary dimension, and it is possible to make some stronger statements when considering specific dimensions. For instance, the counterexample given by Vértesi and Brunner [41] is a two-qutrit state, and hence it would not serve as a counterexample in the 2×2-dimensional case. On the other hand, some other counterexamples such as the Werner state would remain valid in these dimensions.

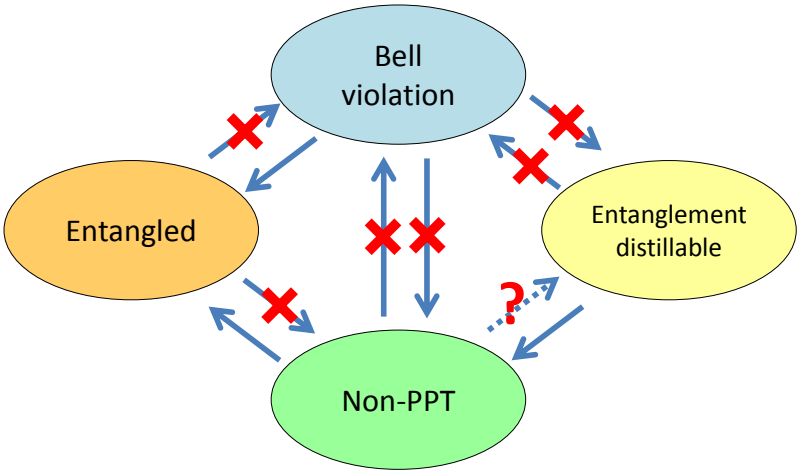

Figure 4.1: Relations between various entanglement-related properties for bipartite states. Whether all bipartite states having non-positive partial transpose are distillable is currently an open question. In the bipartite qubit case, the bottom three conditions of entanglement, distillability and NPPT criterion are all equivalent, and it still holds that Bell violation implies entanglement but not vice versa.

For the case of a two-qubit system, it turns out that these relations are greatly simplified. As stated in Section 1.2.2, a 2×2 state is entangled if and only if it has non-positive partial transpose. Horodecki et al. [32] also showed that any two-qubit entangled state is distillable, and hence distillability is equivalent to entanglement in this case. Therefore, for two-qubit systems the conditions of entanglement, distillability and the NPPT criterion are all equivalent. As for the relation to Bell violations, it still holds that violation of a Bell inequality implies that the state is entangled, and the converse is also still false due to the Werner state $P\left|\Psi\right\rangle\left\langle\Psi\right| + (1-P)\,\mathbb{I}/2^N$ providing a counterexample [42]. Therefore, in the two-qubit case, entanglement, distillability and the NPPT criterion are equivalent, and are a weaker condition than Bell inequality violation.

In light of our earlier observation that the entanglement of GHZ states and Smolin states cannot be detected by one- and two-body correlations, it may be interesting to consider what relationships might hold between these properties and the S2C2M inequalities we have considered. For instance, the fact that Bell inequality violation implies entanglement immediately shows that violation of an S2C2M inequality must imply entanglement as well, since violation of some S2C2M inequality is a stronger condition than violation of some Bell inequality in general. Similarly, the fact that entanglement does not imply Bell inequality violation lets us conclude that it does not imply S2C2M inequality violation either, which can also be explicitly seen from the examples of the GHZ state and Smolin state considered earlier. The case of the Smolin state may also lead to further implications due to the form of bound entanglement that it possesses.

However, in order to discuss the NPPT criterion and distillability for $N \geq 3$ particles, it is necessary to consider how to generalise these concepts, as they originally apply only

to bipartite systems. Some approaches to this include requiring that the NPPT criterion be fulfilled between every pair of particles in the system, or for every possible cut across the system separating it into two subsystems. Similar approaches can be considered for distillability, for instance by defining "N-partite distillability" to mean that a singlet state can be distilled between any pair of particles using LOCC. The relations between Bell inequalities and such multipartite generalisations of these criteria have been studied in some previous works [43], and different choices of generalisation may give rise to different theorems.

We have hence discussed in more detail some of the properties described in Chapter 1, as well as how they are related to each other. Using appropriate generalisations of the NPPT criterion and entanglement distillability, the relations of S2C2M inequality violation with respect to these properties can be considered. In particular, it may be possible that those generalisations requiring conditions to be fulfilled for every pair of particles in the system could be more relevant, because two-body correlations are also obtained from pairs of particles in the system. This would serve as a further development of some of the points explored in this study.

Chapter 5

Conclusion

In this study, we have considered a Bell inequality based on symmetric one- and two-body correlations studied by Tura et al. [12]., comparing it to an entanglement witness $W(k)$ constructed by Krammer et al. [34] as well as the WWZB inequality. By investigating its behaviour with respect to the thermal state of the LMG Hamiltonian, we have shown that the violation of this inequality is relatively weak compared to entanglement detection by $W(k)$ as well as WWZB inequality violation, being less robust against both thermal noise and white noise. As for W states, for the $N > 3$ cases, they do not violate the S2C2M inequality proposed by Tura et al., nor can their entanglement be detected by $W(k)$. A slight generalisation of that S2C2M inequality to allow measurements along arbitrary directions allows it to be violated by such W states, and the WWZB inequality is violated by these states as well. However, the relative quantum violation scales poorly with N. In addition, it was shown that the entanglement of GHZ states and Smolin states cannot violate any Bell inequalities constructed by using only one- and two-body correlations.

We have also investigated the possibility of constructing an entanglement witness based on symmetric one- and two-body correlations, deriving one that is optimal for even numbers of particles. Some properties of this entanglement witness were characterised, such as its detection of $\left|D_N^{\lceil N/2 \rceil}\right\rangle$ Dicke states. It was found that while the entanglement witness is not optimal for odd N, it does become increasingly close to optimal when N is large, apparently causing the trends for odd and even N to converge. As for W states, it is unable to detect their entanglement, though the results from generalising the S2C2M inequality given by Tura et al. suggest that it may be possible to do so by allowing this entanglement witness to make use of measurements along arbitrary directions.

To further develop the results of this study, a number of avenues are possible. For instance, considering the general relations between entanglement, Bell inequality violation, entanglement distillation and the NPPT criterion, one can explore how S2C2M inequalities fit into this framework. Doing so would require generalising the originally bipartite criteria of distillability and the Peres-Horodecki criterion to a multipartite situation, which may be done in several ways. The choice of generalisation used may affect the relations

obtained. In addition, as the entanglement witness derived in this study is non-optimal for odd values of N, it may also be interesting to attempt to improve it to an optimal entanglement witness for such cases. Another way in which it can be generalised would be to allow it to use measurements along arbitrary directions.

Since one- and two-body correlations are more experimentally accessible than higher-order correlations, there is also the possibility of experimentally investigating S2C2M inequalities and entanglement witnesses. Apart from such inequalities, there are also other inequalities that can be constructed from only one- and two-body correlations, such as the translationally invariant Bell inequalities based on such correlations also studied by Tura et al. [35]. It is possible that these classes of inequalities can help to facilitate progress towards further experimental exploration of Bell inequalities and entanglement witnesses.

Bibliography

[1] Bell, J. S. On the Einstein Podolsky Rosen Paradox. *Physics* **1**, 195–200 (1964).

[2] Aspect, A., Grangier, P. & Roger, G. Experimental Realization of Einstein-Podolsky-Rosen-Bohm *Gedankenexperiment* : A New Violation of Bell's Inequalities. *Phys. Rev. Lett.* **49**, 91–94 (1982).

[3] Weihs, G., Jennewein, T., Simon, C., Weinfurter, H. & Zeilinger, A. Violation of Bell's Inequality under Strict Einstein Locality Conditions. *Phys. Rev. Lett.* **81**, 5039–5043 (1998).

[4] Christensen, B. G. *et al.* Detection-Loophole-Free Test of Quantum Nonlocality, and Applications. *Phys. Rev. Lett.* **111**, 130406 (2013).

[5] Brunner, N., Cavalcanti, D., Pironio, S., Scarani, V. & Wehner, S. Bell nonlocality. *Rev. Mod. Phys.* **86**, 419–478 (2014).

[6] Clauser, J. F., Horne, M. A., Shimony, A. & Holt, R. A. Proposed Experiment to Test Local Hidden-Variable Theories. *Phys. Rev. Lett.* **23**, 880–884 (1969).

[7] Mermin, N. D. Extreme quantum entanglement in a superposition of macroscopically distinct states. *Phys. Rev. Lett.* **65**, 1838–1840 (1990).

[8] Ardehali, M. Bell inequalities with a magnitude of violation that grows exponentially with the number of particles. *Phys. Rev. A* **46**, 5375–5378 (1992).

[9] Belinskiĭ, A. V. & Klyshko, D. N. Interference of light and Bell's theorem. *Usp. Fiz. Nauk* **163**, 1–45 (1993).

[10] Werner, R. F. & Wolf, M. M. All-multipartite Bell-correlation inequalities for two dichotomic observables per site. *Phys. Rev. A* **64**, 032112 (2001).

[11] Żukowski, M. & Brukner, Č. Bell's Theorem for General N-Qubit States. *Phys. Rev. Lett.* **88**, 210401 (2002).

[12] Tura, J. *et al.* Detecting nonlocality in many-body quantum states. *Science* **344**, 1256–1258 (2014).

[13] Brans, C. H. Bell's theorem does not eliminate fully causal hidden variables. *Int. J. Theor. Phys.* **27**, 219–226 (1988).

[14] Popescu, S. & Rohrlich, D. Quantum nonlocality as an axiom. *Found. of Phys.* **24**, 379–385 (1994).

[15] Gill, R. D. Time, Finite Statistics, and Bell's Fifth Position. *arXiv:quant-ph/0301059v2* (2015). Accessed on 1 Apr 2015.

[16] Cirel'son, B. S. Quantum generalizations of Bell's inequality. *Lett. Math. Phys.* **4**, 93–100 (1980).

[17] Barrett, J., Hardy, L. & Kent, A. No Signaling and Quantum Key Distribution. *Phys. Rev. Lett.* **95**, 010503 (2005).

[18] Vazirani, U. & Vidick, T. Fully Device-Independent Quantum Key Distribution. *Phys. Rev. Lett.* **113**, 140501 (2014).

[19] Pironio, S., Masanes, L., Leverrier, A. & Acín, A. Security of Device-Independent Quantum Key Distribution in the Bounded-Quantum-Storage Model. *Phys. Rev. X* **3**, 031007 (2013).

[20] Gisin, N. Bell's inequality holds for all non-product states. *Phys. Lett. A* **154**, 201–202 (1991).

[21] Li, M. & Fei, S.-M. Gisin's Theorem for Arbitrary Dimensional Multipartite States. *Phys. Rev. Lett.* **104**, 240502 (2010).

[22] Palazuelos, C. Superactivation of Quantum Nonlocality. *Phys. Rev. Lett.* **109**, 190401 (2012).

[23] Popescu, S. Bell's Inequalities and Density Matrices: Revealing "Hidden" Nonlocality. *Phys. Rev. Lett.* **74**, 2619–2622 (1995).

[24] Liang, Y.-C., Masanes, L. & Rosset, D. All entangled states display some hidden nonlocality. *Phys. Rev. A* **86**, 052115 (2012).

[25] Ekert, A. K. Quantum cryptography based on Bell's theorem. *Phys. Rev. Lett.* **67**, 661–663 (1991).

[26] Bennett, C. H. *et al.* Teleporting an unknown quantum state via dual classical and Einstein-Podolsky-Rosen channels. *Phys. Rev. Lett.* **70**, 1895–1899 (1993).

[27] Bennett, C. H., DiVincenzo, D. P., Smolin, J. A. & Wootters, W. K. Mixed-state entanglement and quantum error correction. *Phys. Rev. A* **54**, 3824–3851 (1996).

[28] Horodecki, M., Horodecki, P. & Horodecki, R. Separability of mixed states: necessary and sufficient conditions. *Phys. Lett. A* **223**, 1–8 (1996).

[29] Terhal, B. M. Bell inequalities and the separability criterion . *Phys. Lett. A* **271**, 319–326 (2000).

[30] Peres, A. Separability Criterion for Density Matrices. *Phys. Rev. Lett.* **77**, 1413–1415 (1996).

[31] Bennett, C. H. *et al.* Purification of Noisy Entanglement and Faithful Teleportation via Noisy Channels. *Phys. Rev. Lett.* **76**, 722–725 (1996).

[32] Horodecki, M., Horodecki, P. & Horodecki, R. Inseparable Two Spin-$\frac{1}{2}$ Density Matrices Can Be Distilled to a Singlet Form. *Phys. Rev. Lett.* **78**, 574–577 (1997).

[33] Horodecki, M., Horodecki, P. & Horodecki, R. Mixed-State Entanglement and Distillation: Is there a "Bound" Entanglement in Nature? *Phys. Rev. Lett.* **80**, 5239–5242 (1998).

[34] Krammer, P. *et al.* Multipartite Entanglement Detection via Structure Factors. *Phys. Rev. Lett.* **103**, 100502 (2009).

[35] Tura, J. *et al.* Translationally invariant multipartite Bell inequalities involving only two-body correlators. *J. Phys. A – Math Gen.* **47**, 424024 (2014).

[36] Lipkin, H., Meshkov, N. & Glick, A. Validity of many-body approximation methods for a solvable model: (I). Exact solutions and perturbation theory. *Nucl. Phys.* **62**, 188–198 (1965).

[37] Castaños, O., López-Peña, R., Hirsch, J. G. & López-Moreno, E. Classical and quantum phase transitions in the Lipkin-Meshkov-Glick model. *Phys. Rev. B* **74**, 104118 (2006).

[38] Żukowski, M., Brukner, Č., Laskowski, W. & Wieśniak, M. Do All Pure Entangled States Violate Bell's Inequalities for Correlation Functions? *Phys. Rev. Lett.* **88**, 210402 (2002).

[39] Greenberger, D. M., Horne, M. A. & Zeilinger, A. Going Beyond Bell's Theorem. *arXiv:0712.0921v1* (2007). Accessed on 20 Dec 2014.

[40] Smolin, J. A. Four-party unlockable bound entangled state. *Phys. Rev. A* **63**, 032306 (2001).

[41] Vértesi, T. & Brunner, N. Disproving the Peres conjecture by showing Bell nonlocality from bound entanglement. *Nat. Commun.* **5** (2014).

[42] Werner, R. F. Quantum states with Einstein-Podolsky-Rosen correlations admitting a hidden-variable model. *Phys. Rev. A* **40**, 4277–4281 (1989).

[43] Acín, A., Scarani, V. & Wolf, M. M. Bell's inequalities and distillability in N-quantum-bit systems. *Phys. Rev. A* **66**, 042323 (2002).

Appendix A

Software and code

Numerical calculations were carried out using the following software:

- The MathWorks, Inc., MATLAB, Version 7.10.0.499, Natick, Massachusetts, United States (2010).
- Wolfram Research, Inc., Mathematica, Version 10.0, Champaign, Illinois, United States (2014).

We also list here the code that was used to generate some of the key data for the figures and tables in this report.

Shown below is the MATLAB code that was used to produce the data for the graphs of $\langle W(0)\rangle$ in Fig. 2.2. Data for the graphs of $\langle B(\theta_{\min})\rangle/B_C$ and $\langle B_W\rangle/2^N$ were computed similarly. The code makes use of a rescaling method we derived to compute the thermal state when the value of T is small, as the exponent in $\rho_T = e^{-H_{LMG}/k_BT}/Z$ becomes very large for such cases. To locate the critical temperatures, this code was first run with the full temperature range for the graphs to identify approximate positions for the roots, then run again with a finer interval spacing in a small range of temperatures near these approximate positions to identify the critical temperatures to higher precision.

```
function krammer_witness()

global basis pauli N kB J B couplingterm fieldterm
basis = {[1; 0], [0; 1]};
pauli = {[0 1; 1 0], [0 -i; i 0], [1 0; 0 -1]};
N = 3; kB = 1; J = 10; B = -.1;
makeplot = 1; writedata = 0;
Tsmall = 0.05; Tmax = 20;

terms = zeros(2^N, 2^N, (N-1)*N/2);
for n = 1:N
```

```
    for m = 1:n-1
        terms(:,:,(n-2)*(n-1)/2+m) = spinops({pauli{1},pauli{1}},[m,n],N)...
            + spinops({pauli{2},pauli{2}},[m,n],N);
    end
end
couplingterm = sum(terms,3);
terms = zeros(2^N, 2^N, N);
for n = 1:N
    terms(:,:,n) = spinops({pauli{3}},[n],N);
end
fieldterm = sum(terms,3);

H = Hlmg(J, B, N);
thmin = acos(ceil(N/2)/(ceil(N/2)+1));

if makeplot==1
    data1name = horzcat('krammer_dat_', num2str(N), 'spin.txt');
    pts = 100;
    left = 0;
    right = Tmax;
    xlist = left + (right-left)*(1:pts)/pts;
    finer = (right-left)/pts*(1:10)/10;
    xlist = [finer xlist];
    ylist = -ones(1,length(xlist));
    witness = wit(0, [1 1 -1], N);
    ptssmall = find(xlist > Tsmall, 1, 'first');
    for n = 1:ptssmall
        s = 1/xlist(n); s = 2*(floor(s/2)) + 1;
        M = -H/(kB*xlist(n)*s);
        eM = expm(M);
        d = eig(eM);
        trscaled = norm(d, s);
        rho = (eM/trscaled)^s;
        ylist(n) = trace(witness*rho);
    end
    for n = ptssmall+1:length(xlist)
        rho = expm(-H/(kB*xlist(n)));
        rho = rho/trace(rho);
        ylist(n) = trace(witness*rho);
    end
    critT = xlist(find(ylist>0, 1, 'first'))
```

```
    fig = figure();
    hold on;
    plot(xlist,ylist);
    plot(xlist,zeros(1,length(xlist)),'k');set(gca,'FontSize',16)
    hold off;
    xlabel('T (Kelvin)');
    ylabel('<W(0)>');
    if writedata == 1
        dlmwrite(data1name, [xlist;ylist]' , 'precision', '%.15f')
    end
end

fprintf('End of run at %s \n', mat2str(clock))

%-------------------------------------------------------------------

function Hlmg = Hlmg(J, B, N)
global couplingterm fieldterm
Hlmg = -J/N*couplingterm - B*fieldterm;

function wit = wit(k, c, N)
sigma = (1/2)*(1/nchoosek(N,2))*(c(1)*(sfac(k, 1, 1, N) + sfac(-k, 1, 1, N))...
    + c(2)*(sfac(k, 2, 2, N) + sfac(-k, 2, 2, N))...
    + c(3)*(sfac(k, 3, 3, N) + sfac(-k, 3, 3, N)));
wit = eye(2^N) - sigma;

function sfac = sfac(k, alpha, beta, N)
global pauli
terms = zeros(2^N, 2^N, (N-1)*N/2);
for n = 1:N
    for m = 1:n-1
        terms(:,:,(n-2)*(n-1)/2+m) = exp(i*k*(n-m))*...
            spinops({pauli{alpha},pauli{beta}},[m n],N);
    end
end
sfac = sum(terms,3);

function otimes = otimes(matrices)
otimes = kron(matrices{1},matrices{2});
for n = 3:length(matrices)
    otimes = kron(otimes,matrices{n});
```

```
end

function ket = ket(bitlist)
global basis
qubits = cell(length(bitlist),1);
for n = 1:length(bitlist)
    qubits{n} = basis{bitlist(n) + 1};
end
ket = otimes(qubits);

function spinops = spinops(ops, pos, N)
oplist = cell(N,1);
idenpos = 1:N; idenpos(pos) = [];
for n = idenpos
    oplist{n} = eye(2);
end
for n = 1:length(pos)
    oplist{pos(n)} = ops{n};
end
spinops = otimes(oplist);
```

Shown below is the Mathematica code that was used to create an approximate plot of the region defined by $A(\theta)$ in correlation space. The number of directions in which it locates a tangent plane can be specified, and it distributes these directions in an approximately uniform fashion using a Fibonacci spiral on the surface of a sphere. The example shown here displays the region for $\theta = \pi/3$, $N = 5$ with 50 tangent planes.

```
fbound[c_, d_, e_, th_, n_] := Module[{a1, a2, a3, l1, l2},
  a1 = c/2 + d*Cos[th] + e/2*Cos[th]^2;
  a2 = d*Sin[th] + e*Sin[th]*Cos[th];
  a3 = e/2*Sin[th]^2;
  l1 = 1/2*(a1 + a3 - Sqrt[a1^2 + a2^2 + a3^2 - 2*a1*a3]);
  l2 = 1/2*(a1 + a3 + Sqrt[a1^2 + a2^2 + a3^2 - 2*a1*a3]);
  Max[{(n^2 - n)*l1, (n^2 - n)*l2, -n*l1, -n*l2}]
  ]

boundverts[th_, n_, numpts_] :=
 Module[{t, phi, c, d, e, matvec, planetrips, nodes, boundpts},
  matvec = Table[
    phi = 1/GoldenRatio*Pi*m;
    t = ArcCos[-1. + 2*m/numpts];
```

```
    c = Sin[t]*Cos[phi]; d = Sin[t]*Sin[phi]; e = Cos[t];
    {c, d, e, fbound[c, d, e, th, n]}
    , {m, numpts}];
  planetrips = Subsets[matvec, {3}];
  nodes =
   Table[Quiet[
     LinearSolve[plane[[All, 1 ;; 3]], plane[[All, 4]]]], {plane,
     planetrips}];
  nodes =
   Select[nodes,
    NumberQ[#[[1]]] && NumberQ[#[[2]]] && NumberQ[#[[3]]] &];
  nodes =
   Transpose[
    Append[Transpose[nodes], ConstantArray[-1, Length[nodes]]]];
  boundpts =
   DeleteDuplicates[(Select[nodes,
       Chop[Max[matvec.Transpose[{#}]]] <= 0 &])[[All, 1 ;; 3]]];
  Return[boundpts]
  ]

ConvexHullMesh[boundverts[Pi/3, 5, 50]]
```